Niche-specific profiling reveals transcriptional adaptations required for the cytosolic lifestyle of *Salmonella enterica*

TuShun R. Powers[a,1], Amanda L. Haeberle[a,1], Disa L. Hammarlöf[b,d], Jennifer A. Cundiff[a], Alexander V. Predeus[b], Karsten Hokamp[c], Jay C.D. Hinton[b], Leigh A. Knodler[a,2]

[1] these authors contributed equally

[2] **Corresponding author:** Leigh A. Knodler PhD, Paul G. Allen School for Global Animal Health, College of Veterinary Medicine, Washington State University, 240 SE Ott Rd, Pullman WA 99164-7090. Email: leigh.knodler@wsu.edu

Short title: Transcriptional profiling of cytosolic *Salmonella*

[a] Paul G. Allen School for Global Animal Health, College of Veterinary Medicine, Washington State University, Pullman, WA 99164-7090, USA

[b] Institute of Infection, Veterinary and Ecological Sciences, University of Liverpool, Liverpool, United Kingdom

[c] Smurfit Institute of Genetics, School of Genetics and Microbiology, Trinity College Dublin, Dublin, Ireland

[d] Present address: SciLifeLab, Science for Life Laboratory, KTH, Sweden

Author contributions: T.R.P. and L.A.K. conceptualization; T.R.P., A.L.H., L.A.K. investigation and methodology; D.L.H. and J.A.C. methodology; A.V.P., L.A.K. visualization; A.V.P., K.H. methodology, formal analysis and data curation; L.A.K., formal analysis; T.R.P., L.A.K., J.C.D.H. funding acquisition; L.A.K. and J.C.D.H. supervision and writing – original draft; T.R.P., A.L.H., D.L.H., J.A.C., A.V.P., K.H. writing – review and editing

Abstract

Salmonella enterica serovar Typhimurium (*S*. Typhimurium) is a zoonotic pathogen that causes diarrheal disease in humans and animals. During salmonellosis, *S*. Typhimurium colonizes epithelial cells lining the gastrointestinal tract. *S*. Typhimurium has an unusual lifestyle in epithelial cells that begins within an endocytic-derived *Salmonella*-containing vacuole (SCV), followed by escape into the cytosol, epithelial cell lysis and bacterial release. The cytosol is a more permissive environment than the SCV and supports rapid bacterial growth. The physicochemical conditions encountered by *S.* Typhimurium within the cytosol, and the bacterial genes required for cytosolic colonization, remain unknown. Here we have exploited the parallel colonization strategies of *S*. Typhimurium in epithelial cells to decipher the two niche-specific bacterial virulence programs. By combining a population-based RNA-seq approach with single-cell microscopic analysis, we identified bacterial genes/sRNAs with cytosol-specific or vacuole-specific expression signatures. Using these genes/sRNAs as environmental biosensors, we defined that *Salmonella* is exposed to iron and manganese deprivation and oxidative stress in the cytosol and zinc and magnesium deprivation in the SCV. Furthermore, iron availability was critical for optimal *S*. Typhimurium replication in the cytosol, as well as *entC*, *fepB*, *soxS* and *sitA-mntH*. Virulence genes that are typically associated with extracellular bacteria, namely *Salmonella* pathogenicity island 1 (SPI1) and SPI4, had a cytosolic-specific expression profile. Our study reveals that the cytosolic and vacuolar *S*. Typhimurium virulence gene programs are unique to, and tailored for, residence within distinct intracellular compartments. Therefore, this archetypical vacuole-adapted pathogen requires extensive transcriptional reprogramming to successfully colonize the mammalian cytosol.

Author Summary

Intracellular pathogens reside either within a membrane-bound vacuole or are free-living in the cytosol and their virulence programs are tailored towards survival within a particular intracellular compartment. Some bacterial pathogens (such as *Salmonella enterica*) can successfully colonize both intracellular niches, but how they do so is unclear. Here we have exploited the parallel intracellular lifestyles of *S. enterica* in epithelial cells to identify the niche-specific bacterial expression profiles and environmental cues encountered by *S. enterica*. We have also discovered bacterial genes that are required for colonization of the cytosol, but not the vacuole. Our results advance our understanding of pathogen-adaptation to alternative replication niches and highlight an emerging concept in the field of bacteria-host cell interactions.

61 **Introduction**

62 There are two major niches in which intracellular bacteria survive and proliferate after
63 internalization into host cells, confined within a membrane-bound vacuole or free-living within the
64 cytosol. Different pathogenic mechanisms are required to occupy these diverse environments.
65 Historically, bacterial pathogens have been categorized as being either vacuolar or cytosolic, but
66 it has recently been realized that some bacteria can occupy both niches, often in a cell-type
67 specific manner. Examples are *Salmonella enterica*, *Mycobacterium tuberculosis* and *Listeria*
68 *monocytogenes* [1–3]. What is unclear is how bacteria that are adapted to survive within one
69 intracellular niche can successfully colonize a distinct cellular compartment.

70 Of the foodborne bacterial, protozoal and viral diseases, non-typhoidal *Salmonella*
71 *enterica* (NTS) cause the largest burden of illness and death worldwide [4]. Infection can cause
72 either a self-limiting gastroenteritis or a life-threatening, invasive disease (invasive non-typhoidal
73 salmonellosis) in immunocompromised individuals, which is particularly a public health problem
74 in sub-Saharan Africa and south-east Asia [5]. Upon ingestion of contaminated food or water, *S*.
75 *enterica* enters epithelial cells lining the gut and resides within a membrane-bound compartment
76 derived from the endocytic pathway [6,7], the *Salmonella*-containing vacuole (SCV). Entry into
77 non-phagocytic cells is largely governed by a type III secretion system, T3SS1, that is encoded
78 by *Salmonella* pathogenicity island (SPI) 1. The T3SS acts as a molecular syringe to inject
79 bacterial effector proteins across the eukaryotic cell plasma membrane to modulate host signaling
80 networks that induce rearrangement of the actin cytoskeleton, leading to the formation of plasma
81 membrane “ruffles” and engulfment of bacteria (reviewed in [8]). Establishment and maintenance
82 of the SCV is dependent upon effectors being translocated across the vacuolar membrane by
83 T3SS1 and another T3SS, T3SS2, which is specifically induced by environmental cues sensed
84 by bacteria within the SCV lumen [9,10]. T3SS2 is also important for survival within phagocytic
85 cells, which *S*. *enterica* encounters in the lamina propria during an enteric infection or in the

86 mesenteric lymph nodes, reticuloendothelial tissues (liver and spleen) and circulating blood during
87 invasive disease.

88 *S. enterica* resides within a membrane-bound vacuole within epithelial cells, fibroblasts,
89 macrophages and dendritic cells (reviewed in [11]). However, the intracellular lifestyle of *S.*
90 *enterica* differs between cell types, with a proportion of the total bacterial population living freely
91 in the cytosol of epithelial cells, a phenomenon described for *Salmonella enterica* serovar
92 Typhimurium (*S*. Typhimurium) and *S*. Typhi infections *in vitro* and/or *in vivo* [12–16]. The
93 eventual outcome of epithelial cells harboring cytosolic bacteria is their expulsion from the
94 monolayer into the lumen of the gut and gall bladder [12,17]; we have proposed that this is a
95 mechanism utilized by *Salmonella* for spreading within and between hosts. Notably, the cytosol
96 of macrophages is not permissive for *S.* Typhimurium replication [18,19], possibly due to nutrient
97 limitation or enhanced host cell innate immune defenses such as autophagy and/or
98 inflammasomes [19]. Considering that the site of intracellular replication is cell-type restricted, we
99 propose that *S. enterica* is an "opportunistic" cytosolic pathogen.

100 A specialized form of autophagy, called xenophagy, protects the mammalian cytosol by
101 targeting intracellular pathogens to autophagosomes for their eventual degradation in lysosomes
102 (reviewed in [20]). In fact, many of the components of the autophagic machinery have been
103 identified using *S*. Typhimurium as a model pathogen. In the first report of autophagic recognition,
104 Brumell and colleagues showed that a sub-population of internalized *S*. Typhimurium damage
105 their nascent vacuole in epithelial cells in a T3SS1-dependent manner and these bacteria are
106 decorated with the autophagy marker, microtubule-associated light chain-3 (LC3) [21]. A recently
107 identified type III effector, SopF, limits the decoration of SCVs with LC3 [22,23]. Damage exposes
108 host glycans restricted to the vacuole lumen to the cytosol, which are then recognized by β-
109 galactoside-binding lectins, specifically galectin-3 (GAL3), GAL8 and GAL9 [24]. Galectin binding
110 acts as an "eat me" signal that initiates a cascade of receptor binding, phagophore formation and
111 tethering to the bacterium, culminating in autophagosome formation [24,25]. However, autophagic

112 control of *Salmonella* is temporal and incomplete, at least in epithelial cells [12,21]. Furthermore,
113 *S*. Typhimurium can also use autophagy to repair damaged SCVs in mouse embryonic fibroblasts
114 [26] and promote replication in the cytosol of epithelial cells [27]. Autophagy therefore serves both
115 a pro- and anti-bacterial role in *S. enterica* infections.

116 Previous studies have largely investigated the infectious cycle of *S*. Typhimurium in
117 epithelial cells by population-based analyses, which do not account for the heterogeneous
118 population of intracellular bacteria. Only by determining the distinct responses of intracellular
119 *Salmonella* to the cytosolic and the vacuolar niche can the infection biology of this important
120 pathogen be accurately defined. Whilst the distinct milieus encountered within a vacuole versus
121 the cytosol provide site-specific cues for *Salmonella* gene induction, little is known about what
122 these cues might be, or which bacterial genes drive replication/survival in the cytosol. Using a
123 combination of RNA-seq-based transcriptomics and single-cell microscopic analysis, here we
124 define the niche-specific environments encountered by *S*. Typhimurium in epithelial cells and
125 identify *S*. Typhimurium genes that are required for bacterial proliferation in the cytosol.

126 **Results**

127 **Modulation of autophagy affects bacterial proliferation in the epithelial cell cytosol.**

128 We hypothesized that the modulation of autophagy in epithelial cells would selectively perturb the
129 cytosolic, and not vacuolar, proliferation of *S*. Typhimurium. Autophagy levels can be manipulated
130 by pharmacological or genetic means (reviewed in [28]). To test our hypothesis, we used nutrient
131 starvation to upregulate autophagy and the class III phosphoinositide 3-kinase (PI3K) inhibitor,
132 wortmannin (WTM), to inhibit autophagy (Fig 1A). To enumerate cytosolic bacteria after
133 autophagy activation/inhibition, we used the digitonin permeabilization assay [12,13] to label the
134 bacteria accessible to cytosol-delivered anti-*S*. Typhimurium lipopolysaccharide (LPS) antibodies
135 at the early stages of infection (15 min – 3 h p.i., Fig 1B). Wild-type bacteria were constitutively
136 expressing *mCherry* from a plasmid, pFPV-mCherry. In untreated cells (basal levels of
137 autophagy), 6.8% of bacteria were accessible to the cytosol as early as 15 min p.i. This proportion
138 increased to ~20% by 45 min p.i. and remained at a steady-state thereafter (Fig 1B). Upon
139 activation of autophagy (EBSS), the fraction of bacteria that were accessible to the cytosol was
140 reduced at 45 min, 90 min and 180 min p.i. (Fig 1B), consistent with enhanced autophagic capture
141 of bacteria in, or repair of, damaged vacuoles. In contrast, inhibition of autophagy (WTM)
142 increased the proportion of cytosolic bacteria at all timepoints examined (Fig 1B), in agreement
143 with previous findings [14,29].

144 To verify cytosolic localization, we used a transcriptional reporter plasmid, pNF101, that
145 only expresses *gfp-ova* in the sub-population of *S*. Typhimurium that are in damaged vacuoles
146 and/or free in the cytosol. Epithelial cells were infected with mCherry-*S*. Typhimurium (*S*.
147 Typhimurium wild-type bacteria constitutively expressing *mCherry* on the chromosome) harboring
148 pNF101. In untreated cells, 35% and 13% of infected cells harbored GFP-positive (cytosolic)
149 bacteria at 2 h and 8 h p.i., respectively (Fig 1C). EBSS treatment lowered this proportion at both
150 timepoints to 23% and 8%, respectively. Conversely, WTM treatment increased the level of
151 infected cells with cytosolic bacteria at both 2 h and 8 h p.i. (79% and 48%).

152 To quantify the niche-specific effects of EBSS and WTM treatments on bacterial
153 replication, epithelial cells were infected with *S*. Typhimurium harboring pFPV-mCherry and the
154 number of bacteria per cell was scored. Cytosolic *S*. Typhimurium that evade autophagic
155 clearance replicate at a much faster rate than vacuolar bacteria in epithelial cells [12,13,30],
156 eventually occupying the entire cytosolic space (≥100 bacteria/cell). By contrast, vacuolar bacteria
157 display low to moderate replication (2-40 bacteria/cell). Comparing the three treatment conditions,
158 the incidence of infected cells with ≥100 bacteria at 8 h p.i. (8.2±1.6% in control, n=3 experiments)
159 was reduced by EBSS treatment (1.2±2.0%) and promoted by WTM treatment (16±5.4%) (Fig
160 1D). Neither bacterial invasion at 1 h p.i. nor vacuolar replication at 8 h p.i. was overtly affected
161 (Fig 1D). In agreement, total bacterial proliferation was restricted and promoted by EBSS and
162 WTM treatment, respectively, compared to untreated cells (Fig 1E). Collectively, these data
163 confirm that modulation of autophagy selectively affects the proliferation of *S*. Typhimurium in the
164 cytosol of epithelial cells.
165
166 **Identification of cytosol- and vacuole-specific genes by RNA-seq analysis.**
167 To define the transcriptional signature of cytosolic *S*. Typhimurium, we isolated bacterial RNA
168 from epithelial cells that had been enriched for either cytosolic or vacuolar S. Typhimurium by
169 EBSS- or WTM-treatment, respectively, for transcriptomic analysis. Treated cells were infected
170 with wild-type bacteria (Fig 1A), samples were collected and processed at 8 h p.i. and bacterial
171 RNA was extracted using an enrichment protocol described previously ([31]; Fig S1). Four cDNA
172 libraries were derived from two biological replicates and analyzed by RNA-seq (see Materials and
173 Methods; [32]). The entire dataset is available in Dataset S1 and includes the expression profiles
174 of the 4,742 coding genes and 280 sRNA identified previously in *S*. Typhimurium SL1344 [32,33].
175 We defined genes/sRNAs as preferentially induced in the cytosol ("up cytosol", WTM/EBSS
176 ≥1.40-fold change) and vacuole ("up vacuole", WTM/EBSS ≤0.61-fold change), respectively, and

177 identified 113 statistically-significant “up cytosol” genes/sRNAs and 242 “up vacuole”
178 genes/sRNAs (Dataset S1).

179 Of the twelve chromosomally-encoded pathogenicity islands (PAIs) in *S*. Typhimurium, only
180 four were up-regulated in the cytosolic environment (Fig S2). Most obvious was the abundance
181 of SPI1 genes that were up-regulated, consistent with the reported induction of *prgH* in the
182 cytosolic population at later times in epithelial cells [12,34]. SPI4, which encodes a giant non-
183 fimbrial adhesin and its cognate type I secretion system and is co-regulated with SPI1 [35,36],
184 was also up-regulated in the cytosol. Lastly, genes encoding for two T3SS1 effectors within SPI5
185 and SPI11, SopB [37,38] and SopF [22,23,39], respectively, were up-regulated in cytosolic
186 bacteria. The remaining SPI5 and SPI11 genes were either up-regulated in the vacuolar
187 population, or had unchanged expression, highlighting the mosaic nature of PAIs. Most SPI2
188 genes were up-regulated in the vacuolar population, as were genes encoding two type III effectors
189 translocated by T3SS2 (*pipB* in SPI5 and *sspH2* in SPI12). SPI3 genes were up-regulated in the
190 SCV of epithelial cells, like in macrophages [40,41]. Similarly, most genes within SPI11, a PAI
191 that is important for macrophage survival [42], and SPI12 were up-regulated in the epithelial SCV.
192 The majority of SPI6 genes (which encode a type VI secretion system; [43]), all SPI9 genes
193 (encode a type I secretion system; [44]) and SPI16 genes were not expressed in bacteria residing
194 within either niche in epithelial cells. Overall, the transcriptional signatures of cytosolic and
195 vacuolar bacteria at the PAI level (Fig S2) validates the basis of our RNA-seq analysis.

196 To put the observed gene expression changes into the context of the extensive *S. enterica*
197 literature, we used an innovative approach that involved the curation of 80 custom pathways from
198 previously published regulons that had been defined by RNA-seq, ChIP-seq or microarray-based
199 analysis. We combined these pathways with KEGG and GO gene sets to annotate the subsets of
200 “up cytosol” and “up vacuole” *S*. Typhimurium genes/sRNAs (Fig 2; Dataset S2). The list of “up
201 vacuole” genes/sRNAs included an abundance (e.g. SPI2, *pipB*, *pgtE*, PinT, InvS, *steB*) that are
202 positively regulated by the two-component systems that govern SPI2 induction in the SCV,

203 namely PhoPQ, SsrAB and OmpRZ. Conversely, genes/sRNAs that are negatively regulated by
204 these two component systems were in the “up cytosol” category. The SPI1-encoded transcription
205 factors, HilA, HilD, and InvF, are required for the expression of SPI1 genes [45], and accordingly
206 many of the “up cytosol” genes/sRNAs (e.g. *sipBCDA*, *siiCD*, *sopF*, *sopB*) grouped with these
207 regulons. Our analysis also revealed many specific gene signatures (Fig 2). For example, genes
208 associated with iron transport were solely up-regulated in the cytosol. Up-regulation of the
209 tricarboxylic acid (TCA) cycle, lysine degradation and molybdate transport was evident in vacuolar
210 bacteria, suggesting increased reliance of *Salmonella* on these energy sources in the SCV.
211 Interestingly, genes/sRNAs that are repressed by Ferric uptake regulator (Fur) in iron-replete
212 conditions and activated by Hfq, BarA/SirA and FliZ were up-regulated in both the vacuole and
213 cytosol.

214 We used the expression profiles of *S*. Typhimurium grown in 22 distinct infection-relevant
215 *in vitro* growth conditions [32] to predict the environmental conditions experienced by *S*.
216 Typhimurium when in the cytosol and vacuole. For the 113 genes/sRNAs up-regulated in the
217 cytosol, three main patterns emerged: (i) up-regulation by bile shock (3% bile for 10 min) and/or
218 low Fe^{2+} shock (200 μM 2,2-dipyridyl (DPI) for 10 min) (e.g. *mntH*, *sitABCD*, *entCEBA*), (ii) up-
219 regulation by NaCl shock (0.3 M NaCl for 10 min) (e.g. *proVW*, *ilvX*), (iii) up-regulation during late
220 exponential/early stationary phase of growth (e.g. *sopE2*, *sipBCDA*, *siiABCDEF*) (Dataset S1).
221 This suggests that cytosolic bacteria are growing fast and exposed to a low iron, high osmolarity
222 physicochemical environment. The rapid growth of cytosolic *S*. Typhimurium has been previously
223 observed [12,13,30], validating the latter prediction. A common theme observed for the 242
224 genes/sRNAs up-regulated in the vacuole was induction by: (i) *in vitro* SPI2 growth conditions
225 and/or (ii) internalization into macrophages (Dataset S1).

226

227 **Cytosolic iron-limitation is a cue for *S*. Typhimurium gene/sRNA induction**

228 To validate the cytosolic expression of genes/sRNAs predicted by RNA-seq analysis using
229 *gfpmut3* transcriptional fusions because green fluorescent protein (GFP) is an ideal reporter to
230 study differential gene expression in individual bacteria in infected host cells and tissues
231 [12,17,46,47]. Previously *gfpmut3* transcriptional fusions have demonstrated the vacuole-specific
232 induction of SPI2 genes [48], for example. We initially focused on those genes/sRNAs that are
233 induced when *Salmonella* are exposed to low Fe^{2+} and/or bile shock in broth [32] (Dataset S1).
234 Epithelial cells were infected with mCherry-*S*. Typhimurium carrying individual *gfpmut3* reporters
235 and bacterial GFP fluorescence intensity was assessed qualitatively and quantitatively at 8 h p.i.
236 The following genes/sRNAs were confirmed to be up-regulated in the cytosol: *entC* (*entCEBA*
237 operon), *fepA* (*fepA-entD* operon), *fepB*, *fhuA* (*fhuACBD* operon), *fhuE*, *iroB* (*iroBCDE* operon),
238 *iroN*, *mntH*, *nrdH* (*nrdHIEF* operon), *sitA* (*sitABCD* operon), SL1802, SL3990 (SL3990-SL3989
239 operon), *sufA* (*sufABCDSE* operon), *yjjZ* (SL1344_4483), STnc3080 and STnc3250 (Fig 3, upper
240 panels; Fig S3). Up-regulation of STnc4000, *ilvC* and SL1344_2715 was not observed by
241 fluorescence microscopy (Fig S6). Quantification using ImageJ software of the mean
242 fluorescence intensity (MFI) of the GFP signal associated with individual bacteria confirmed the
243 qualitative analysis for *iroB* (11.2-fold increase in MFI for cytosolic bacteria), *nrdH* (10.6-fold), *sitA*
244 (13.3-fold), *sufA* (Fig 6.2-fold), *yjjZ* (23.2-fold) and STnc3080 (11.1-fold) (Fig 3, lower panel).
245 All of the confirmed genes/sRNAs are up-regulated by “low Fe2+ shock” in broth (addition
246 of 200 μM DPI for 10 min (35)). DPI chelation is not specific to iron, however [49,50], raising the
247 possibility that other metals also regulate the expression of these genes/sRNAs. We used *iroN*,
248 *sitA*, *yjjZ*, *sufA*, *fepA* and STnc3250 promoters to determine metal cation specificity *in vitro*. The
249 effect of increasing concentrations (0.1-100 μM) of Co^{2+}, Fe^{3+}, Mn^{2+}, Ni^{2+} or Zn^{2+} on GFP
250 fluorescence for bacteria grown in defined minimal media (M9) was measured (Fig S4). For all
251 reporters, maximal expression was observed in the absence of metal addition. Upon addition of
252 Fe^{3+} and Co^{2+}, GFP expression of *S*. Typhimurium carrying P*iroN-gfpmut3*, P*yjjZ-gfpmut3* and
253 P*fepA-gfpmut3* reporters decreased in a dose-dependent manner. Notably, the promoter

254 responses were 10- to 100-fold more sensitive to Fe^{3+} than Co^{2+}. P*sitA-gfpmut3* expression was
255 modulated by Fe^{3+}, Mn^{2+} and Co^{2+}, although Fe^{3+} and Mn^{2+} were clearly the most potent
256 repressors by an order of magnitude, in agreement with a previous study using a *sitA*::*lacZ*
257 reporter [51]. Lastly, expression of P*STnc3250-gfpmut3* and P*sufA-gfpmut3* were only reduced
258 by increased concentrations of Fe^{3+}. P*iroN-gfpmut3* was the most sensitive iron reporter, with a
259 >50% reduction in fluorescence at 0.1 μM Fe^{3+}. Collectively, the *in vitro* repression of these
260 genes/sRNAs by 0.1-1 μM Fe^{3+} hinted that the cue for cytosol-specific induction was iron limitation
261 (<0.1 μM).

262 To test the response of reporters to iron concentrations during infection, we used ferric
263 ammonium citrate (FAC) to increase free iron levels in mammalian cells [52,53]. Epithelial cells
264 were incubated overnight in growth media containing increasing concentrations (10-300 μM) of
265 FAC. Untreated and FAC-treated cells were infected with mCherry-*S*. Typhimurium carrying
266 transcriptional reporters, fixed at 8 h p.i. and the MFI of GFP signal for cytosolic and vacuolar
267 bacteria quantified by fluorescence microscopy and ImageJ (Fig 4). The MFI of cytosolic bacteria
268 harboring P*iroN-gfpmut3*, P*sitA-gfpmut3* or P*yjjZ-gfpmut3* reporters was reduced in a dose-
269 dependent manner over the FAC concentration range. Specifically, fluorescence was reduced by
270 56.7-, 35.9- and 14.5-fold, respectively, upon the addition of 300 μM FAC to growth media (Fig
271 4A), indicating repression of *iroN*, *sitA* and *yjjZ* expression in the cytosol under iron-replete
272 conditions. The low MFI for vacuolar bacteria in untreated cells limited our analysis of the iron-
273 dependent repression of *iroN*, *sitA* and *yjjZ* in the SCV.

274 We used the lipophilic, cell-permeable chelator, DPI, as an independent way to assess the
275 effects of metals on *S*. Typhimurium gene expression in the mammalian cytosol. Because DPI
276 has a high affinity for various metal cations, we assessed the specificity for iron by means of an
277 "add-back" experimental design [49,54,55] whereby an equimolar amount of Fe^{3+} was added to
278 the DPI-treated media. Epithelial cells were treated overnight with 200 μM DPI, 200 μM DPI plus
279 200 μM FAC, or 200 μM FAC alone and infected with mCherry-*S*. Typhimurium harboring P*iroN-*

280 *gfpmut3*, P*sitA-gfpmut3* or P*yjjZ-gfpmut3* reporters. Cells were fixed at 8 h p.i. and the intensity
281 of GFP signal for cytosolic and vacuolar bacteria quantified via fluorescence microscopy. Addition
282 of DPI increased the expression of *iroN*, *sitA* and *yjjZ* for both cytosolic and vacuolar bacteria (Fig
283 4B), indicating that DPI accesses both cellular compartments. However, the effects of divalent
284 cation chelation were more pronounced for the vacuolar population (13- to 43-fold increase in
285 MFI) than the cytosolic population (1.7- to 2.2-fold increase in MFI). Add-back of iron restored the
286 MFI to that of untreated cells for cytosolic bacteria harboring P*iroN-gfpmut3* and P*sitA-gfpmut3*
287 reporters (Fig 4B), demonstrating that iron limitation is the primary stimulus for the up-regulation
288 of these genes in the cytosol. Add-back of iron had negligible effects on the MFI of bacteria
289 harboring the P*yjjZ-gfpmut3* reporter, regardless of their intracellular niche (Fig 4B), possibly due
290 to a lower sensitivity of *yjjZ* to changes in free iron levels (Fig 4A) or a responsiveness to
291 deprivation of metals other than iron in the intracellular environment (Fig S4). Add-back of iron
292 only partially restored the expression of *sitA* and *iroN* in vacuolar bacteria (Fig 4B) suggesting
293 that *sitA* and *iroN* respond to multiple divalent cations in the SCV or FAC treatment does not
294 significantly increase free iron levels in endocytic-derived compartments. Taken together, our
295 data show that iron limitation in the mammalian cytosol is a major cue sensed by *S*. Typhimurium.
296 Using the same treatment conditions, we determined the role of iron limitation on bacterial
297 replication in epithelial cells. As assessed by gentamicin protection assay (Fig 4C), total bacterial
298 replication was limited by treatment with DPI (4.0-fold replication over 8 h) and DPI plus FAC (5.6-
299 fold), but not FAC alone (8.8-fold), compared to untreated cells (10.0-fold). The chloroquine
300 (CHQ) resistance assay, which quantifies the proportion of cytosolic bacteria in the total
301 population, showed a similar profile (Fig 4D). Compared to untreated cells at Fig 6 h p.i (50±3.4%
302 cytosolic bacteria), treatment with DPI reduced the levels of cytosolic bacteria to 28±6.Fig 6%.
303 The proportion of cytosolic bacteria was increased to 42±11% upon add-back of iron (DPI+FAC),
304 whereas it was indistinguishable from untreated cells for FAC alone (52±5.5% cytosolic).

305 It has been shown that epithelial cells contain either cytosolic bacteria, vacuolar bacteria
306 or a mix of both populations at later times p.i. [30]. We used single-cell analysis to monitor the
307 effect of metals on the distribution of these intracellular populations. Using mCherry-*S*.
308 Typhimurium harboring pFN101 as a fluorescent reporter for cytosolic access, we analyzed the
309 intracellular populations at 8 h p.i., in addition to the number of cytosolic (GFP+, mCherry+) and
310 vacuolar (GFP-, mCherry+) bacteria within each infected cell. There was no significant difference
311 in the frequency of epithelial cells that only contained cytosolic bacteria (0-1.2% of infected cells),
312 only vacuolar bacteria (84.0-86.4% of infected cells) or a mixed population (12.4-16.0% of infected
313 cells) between any of the treatments (Fig 4E, left panel), indicating that metal chelation does not
314 alter the intracellular distribution of bacteria. However, the ability of *Salmonella* to replicate in the
315 cytosol was noticeably affected (Fig 4E, right panel), in agreement with the CHQ resistance assay
316 results. In untreated (control) cells, 6.4±0.89% of infected cells contained ≥100 cytosolic
317 bacteria/cell. DPI treatment reduced proliferation of *S*. Typhimurium in the cytosol such that only
318 0.40±0.89% of infected cells contained ≥100 cytosolic bacteria/cell ($p<0.05$, $n\geq4$ experiments).
319 Add-back of iron (DPI+FAC) partially restored the hyper-proliferative capacity of *S*. Typhimurium
320 in the cytosol (3.3±1.9%; $p<0.05$ compared to untreated, $n\geq4$ experiments) whereas FAC
321 treatment alone (7.8±1.7%) was no different than control. DPI also limited bacterial replication in
322 the SCV (Fig 4E, right panel) as evidenced by a reduction in the mean number of vacuolar
323 bacteria/cell at 8 h p.i. (14.0 for untreated and 10.4 for DPI-treated, $p<0.05$, $n\geq5$ experiments).
324 Add-back of iron restored vacuolar replication (12.5 bacteria/cell) whereas FAC alone (11.5
325 bacteria/cell) was not significantly different to untreated cells. In summary, iron restriction affects
326 *S*. Typhimurium proliferation in both the cytosol and vacuole in epithelial cells but has a more
327 profound effect in the cytosol.
328
329 **Zinc and magnesium are limiting in the vacuole but not the cytosol.**

330 We investigated whether metals other than iron affected intracellular *S*. Typhimurium gene
331 expression in epithelial cells. *S*. Typhimurium encodes multiple transporters for divalent cations
332 [56]. The up-regulation of *sitA* and *mntH* in cytosolic *S*. Typhimurium (Fig 3; Fig S3), which are
333 induced by iron and manganese limitation (Fig S4) [51,54] and encode high affinity Mn^{2+}
334 transporters [57,58], suggests that Mn^{2+} availability is low in the cytosol. Zn^{2+} transport in *S*.
335 Typhimurium is dependent on a high affinity transport system, ZnuABC [59], and its accessory
336 protein, ZinT [60,61], and a low affinity ZIP family metal permease, ZupT [62,63]. *zupT* is
337 constitutively expressed [62], in agreement with our RNA-seq analysis (Dataset S1). By contrast,
338 *znuA* and *zinT* are induced when zinc is limiting [64] and both genes are in the "up vacuole"
339 shortlist (Dataset S1). We found that a P*zinT-gfpmut3* reporter was exquisitely sensitive to zinc
340 concentrations, with a 54% and 99% reduction in GFP fluorescence observed upon the addition
341 of 0.1 μM and 1 μM Zn^{2+} to minimal media, respectively (Fig S4). When epithelial cells were
342 infected with mCherry-*S*. Typhimurium harboring P*zinT-gfpmut3*, GFP fluorescence was evident
343 in vacuolar, but not cytosolic, bacteria at 8 h p.i. (Fig 5), indicating that low-zinc conditions prevail
344 in the SCV (<0.1 μM). Quantification of the MFI of the GFP signal associated with individual
345 bacteria confirmed the qualitative findings (5.8-fold increase in vacuole; Fig 5, lower panel).
346 *S.* Typhimurium also multiple Mg^{2+} transporters. CorA is a constitutively expressed Mg^{2+}
347 transporter, and MgtA and MtgB are inducible Mg^{2+} transporters [65]. Consistent with its
348 constitutive expression, expression of *corA* was similar in both vacuolar and cytosolic bacteria
349 (Dataset S1). Low Mg^{2+} induces *mgtA* and *mgtB* transcription [65,66]. Expression of *mgtA* was
350 not induced in the vacuole, however (Dataset S1). Acidic pH abolishes the *mgtA* (but not *mgtB*)
351 transcriptional response to Mg^{2+} concentration [66], which could explain why *mgtA* is not induced
352 in the SCV of epithelial cells. In contrast, all three genes within the *mgtCBR* operon were up-
353 regulated in vacuolar bacteria according to the RNA-seq data (Dataset S1). Using mCherry-*S*.
354 Typhimurium harboring P*mgtC-gfpmut3*, we confirmed *mgtCBR* is responsive to Mg^{2+} levels (Fig
355 S4) and the operon is specifically up-regulated in the SCV (Fig 5). The MFI of GFP signal was

356 increased by 6.2-fold for vacuolar bacteria (Fig 5, lower panel). Altogether, our studies of Zn^{2+}
357 and Mg^{2+} transporters reveal that levels of these cations are more limiting in the SCV than the
358 cytosol.
359
360 **Confirmation of growth-phase related, cytosol-specific genes.**
361 Our transcriptomic analysis highlighted another set of cytosol-induced genes that were highly
362 expressed during late exponential/early stationary phase of *in vitro* growth in broth, and in some
363 cases responsive to oxygen shock (Fig 2; Dataset S1). Many of the genes encode for T3SS1
364 structural proteins (*orgA*, *spaQ*, *sipB*, *sipC*, *sipD*) and effectors known to be translocated by
365 T3SS1 (*sipA*, *sopB*, *sopD*, *sopE*, *sopE2*, *sopF* [SL1344_1177]). Using GFP transcriptional
366 reporters, we confirmed the cytosol-specific induction of *sicA* (*sicA-sipBCDA* operon), *sopE2* and
367 *sopF* (Fig 6). We have previously shown that *prgH* (*prgHIJK-orgABC* operon), encoding a
368 structural T3SS1 component, is up-regulated in cytosolic bacteria [12], in agreement with our
369 RNA-seq results (Dataset S1). PipB, a T3SS2 effector encoded on SPI5 [67], was used as a
370 control for the vacuole-specific induction of a type III effector. GFP fluorescence was only detected
371 for vacuolar bacteria harboring a P*pipB-gfpmut3* reporter (Fig 6). We confirmed that *siiA*
372 (*siiABCDEF* operon) and *lpxR* also showed cytosol-specific expression (Fig 6). The *siiABCDEF*
373 operon in SPI4 (Fig S2) encodes for a type I secretion system for the secretion of SiiE, a giant
374 non-fimbrial adhesin [68,69]. Immunostaining with anti-SiiE antibodies detected the adhesin on
375 the surface of cytosolic bacteria (Fig S5, upper panel), and diffusely spread throughout the cytosol
376 (Fig S5, lower panel). Vacuolar bacteria were negative for SiiE staining (Fig S5). We have
377 previously shown by electron microscopy that cytosolic bacteria have extensive filamentous
378 material on their surface [12]. Taken together, our findings suggest the filaments could be SiiE.
379 Like *siiABCDE*, *lpxR* (SL1344_1263) is also co-regulated with SPI1 [70] and encodes a
380 hypothetical outer membrane protein. Transcriptional reporters did not verify cytosolic up-
381 regulation of *ygbA* (SL1344_2840), which encodes a conserved hypothetical protein required for

382 *S*. Typhimurium growth during nitrosative stress [71], or *asnA*, which is involved in asparagine
383 biosynthesis [72] (Fig S6).

384 We conclude that there is a generalized up-regulation of "SPI1 associated" genes in the
385 mammalian cytosol. However, we do not observe uniform up-regulation of these genes within the
386 cytosolic population (Fig 6), in agreement with previous reports for *prgH* [12,14,34], which is
387 different than that observed for the iron-responsive cytosol-specific genes/sRNAs (Fig 3). Such
388 heterogeneity was verified by ImageJ quantification of the MFI of GFP signal associated with
389 individual bacteria carrying P*sicA-gfpmut3*, P*sopE2-gfpmut3*, P*sopF-gfpmut3*, P*siiA-gfpmut3* or
390 P*lpxR-gfpmut3* reporters. All genes were more highly expressed in cytosolic bacteria (Fig Fig 6,
391 lower panel) – *sicA* (2.6-fold), *sopE2* (6.0-fold), *sopF* (3.7-fold), *siiA* (8.7-fold) and *lpxR* (2.3-fold)
392 – yet with broader variability in MFI/bacterium than the iron-regulated genes (Fig 3), and with
393 many cytosolic bacteria having background levels of GFP fluorescence.

394

395 **Extraneous genes that belong to the cytosol-specific program.**

396 Several osmotically-sensitive genes that are up-regulated when *S*. Typhimurium is exposed to
397 NaCl shock [32] were identified as candidate cytosol-specific genes, namely *cysP* (*cysPUWA*
398 operon), *soxS* and *proV* (*proVWX* operon) (Dataset S1). We qualitatively and quantitatively
399 confirmed the cytosol-specific expression of *cysP* and *soxS* using transcriptional reporters (Fig
400 S7). However, the *proV-gfpmut3* transcriptional fusion was not up-regulated in the cytosol (Fig
401 S6). The *cysPUWA* operon encodes a sulfate/thiosulfate permease and periplasmic binding
402 protein [73]. SoxS is a member of the AraC/XylS family of transcriptional regulators that is required
403 for bacterial resistance to oxidative stress [74,75].

404 Four additional *S*. Typhimurium genes were identified as being up-regulated in the cytosol
405 according to the transcriptomics data, namely *uhpT*, *sfbA* (*sfbABC* operon), *mtr* and *trpE*
406 (*trpEDCBA* operon) (Dataset S1). All four genes are constitutively expressed in infection-relevant
407 broth conditions [32], and *sfbA*, *mtr* and *trpE* are also up-regulated upon infection of macrophages

408 ([41]; Dataset S1). Infection of epithelial cells with mCherry-*S*. Typhimurium harboring P*uhpT-*
409 *gfpmut3* or P*sfbA-gfpmut3* confirmed the RNA-seq-based prediction of their cytosol-specific
410 induction (Fig S7). However, *mtr* and *trpE* were not induced in the cytosol (Fig S6). UhpT is a
411 hexose phosphate transporter whose induction has been reported previously for cytosolic *S*.
412 Typhimurium [34]. The *sfbABC* operon is predicted to encode a periplasmic iron-binding
413 lipoprotein SfbA, a nucleotide-binding ATPase SfbB and a cytoplasmic permease SfbC [76].
414
415 **Identification of *S*. Typhimurium genes required for optimal cytosolic proliferation.**
416 Having identified *S*. Typhimurium genes/sRNAs that are specifically up-regulated within the
417 epithelial cytosol, we next tested whether any of these genes/sRNAs are required for colonization
418 of this niche. We did not focus on the SPI1-associated effectors as their individual contributions
419 to the cytosolic stage of the intracellular cycle have been reported previously [22,30,77,78].
420 Eighteen gene deletion mutants were constructed and their ability to access and replicate within
421 the cytosol was first assessed in a population-based assay by CHQ resistance. We identified five
422 genes required for cytosolic replication in epithelial cells, namely *entC*, *fepB*, *sitA, mntH* and *soxS*.
423 Deletion of these genes led to a reduced proportion of cytosolic bacteria at 7 h p.i. (42.5% for
424 Δ*entC*, 41.9% for Δ*fepB*, 40.1% for Δ*mntH*Δ*sitA* and 42.6% for Δ*soxS*; Fig 7A). The remaining
425 mutants had similar proportions of cytosolic bacteria as wild-type S. Typhimurium (50.2%, Fig
426 7A).
427 We extended this population-based assay with single-cell analysis using *S*. Typhimurium
428 harboring the dual fluorescence reporter plasmid, pCHAR-Duo(ASV), in which constitutive
429 expression of *mCherry* is driven by the synthetic promoter ProB and destabilized GFP
430 (*gfpmut3.1(ASV)*) is under the control of the *S*. Typhimurium *uhpT* promoter. All bacteria
431 harboring this plasmid are mCherry-positive and only those bacteria in the cytosol will be GFP-
432 positive. Epithelial cells were infected with wild-type, Δ*entC*, Δ*fepB*, Δ*sitA*Δ*mntH* or Δ*soxS* bacteria
433 harboring pCHAR-Duo(ASV) and the number of infected cells containing only cytosolic bacteria,

434 only vacuolar bacteria or a mixed population (cytosolic and vacuolar) at 8 h p.i. was scored by
435 fluorescence microscopy. For all the deletion mutants, we detected fewer infected epithelial cells
436 in the mixed population category than for wild-type bacteria (Fig 7B). Furthermore, fewer infected
437 cells contained ≥100 cytosolic bacteria at 8 h p.i. (wild-type bacteria = 6.25%, Δ*entC* = 3.75%,
438 Δ*fepB* = 5.0%, Δ*sitA*Δ*mntH* = 4.0% and Δ*soxS* = 4.0%; n=4 experiments). Altogether, these results
439 identify *entC*, *fepB*, *sitA-mntH* and *soxS* as being specifically required for the optimal proliferation
440 of *S*. Typhimurium in the cytosol of epithelial cells.

441

442 **Discussion**

443 Compared to an endocytic-derived vacuole, the host cell cytosol could naïvely be viewed as a
444 nutrient-rich milieu that allows for the efficient growth of bacteria. However, not all pathogens can
445 survive within this niche, and *S*. Typhimurium can only replicate in the cytosol of epithelial cells
446 and certain embryonic fibroblast lines [12,14,19]. Our findings that vastly different virulence gene
447 programs are activated when *S*. Typhimurium colonizes the SCV and cytosol confirm previous
448 suggestions that the mammalian cytosol is a complex environment that requires pathogen-
449 specific adaptations for efficient bacterial survival and replication [79].

450 Here we report the "cytosol transcriptional signature" of bacteria by integrating our data
451 with the available gene expression profiles of Gram-negative pathogens that colonize the cytosol
452 (Table 1). We focus on the prototypical cytosolic pathogen, *S. flexneri* [80,81], and uropathogenic
453 *Escherichia coli* (UPEC) [82,83], which forms intracellular bacterial communities (IBCs) in the
454 cytosol of bladder epithelial cells. The most striking feature that emerges is the enrichment of
455 genes that mediate the acquisition of iron (Table 1). *Salmonella* acquires ferric (Fe^{3+}) iron by
456 secreting two siderophores, enterobactin and salmochelin, a C-glucosylated form of enterobactin
457 [56,84,85]. Iron-loaded siderophores then transit back into bacteria by first binding the outer
458 membrane receptors, FepA and IroN [86,87], then FepB in the periplasm, and finally across the
459 cytoplasmic membrane via the ABC-type transporter, FepDGC [88]. FhuE, FhuA and FoxA also
460 function as outer membrane receptors to exploit the utilization of ferric siderophores produced by
461 other bacteria [89]. All of the siderophore synthesis and transport loci are up-regulated in cytosolic
462 *S*. Typhimurium (Table 1, Fig 2). *S. flexneri* uses a similar strategy involving the synthesis of
463 another siderophore, aerobactin [90], and the genes required for aerobactin synthesis and binding
464 (*iucABCD* operon) are highly up-regulated in the cytosol (Table 1). The limited data available for
465 UPEC IBCs are consistent with an important role of ferric iron acquisition for this bacterium (Table
466 1). Genes encoding the ferrous (Fe^{2+}) iron transport systems of *S. flexneri* (*feoB*, *sitABCD* and
467 *mntH*) and *S*. Typhimurium (*sitABCD* and *mntH*) are also up-regulated, but not *feoB* (Table 1).

468 The Sit and MntH systems in *S*. Typhimurium transport both ferrous iron and manganese, but
469 likely function as manganese transporters under physiological conditions [57,58]. We found that
470 a *S*. Typhimurium Δ*sitA*Δ*mntH* mutant is compromised for growth in the epithelial cytosol (Fig 7),
471 indicating a specific requirement for Mn^{2+} acquisition in this compartment, but the same transport
472 systems do not contribute to the growth of *S. flexneri* in epithelial cells [91]. The panopoly of iron
473 acquisition systems used by enteric bacteria means that genetic deletions in multiple pathways
474 are required to affect intracellular proliferation. For example, single gene deletions of *sitA*, *iucB* or
475 *feoB* in *S. flexneri* have no effect on intracellular growth but a mutant in all three genes is unable
476 to grow [92]. Similarly, *S*. Typhimurium Δ*entC* (defective in the synthesis of enterobactin and
477 salmochelin; [93]) and Δ*fepB* (defective for the import of enterobactin, salmochelin and
478 catecholate breakdown products containing iron; [84]) mutants fail to proliferate in the epithelial
479 cytosol (Fig 7).

480 Table 1: Cytosol signature genes

Gene	**Function**	**Up-regulated in epithelial cytosol?**		
		***S*. Typhimurium**	***S. flexneri*[a,b,c]**	**UPEC[d,e]**
bioA	Biotin synthesis	No	Yes	
cysP	Thiosulfate binding protein	Yes	No (downregulated)	
entC	Siderophore biosynthesis	Yes	Pseudogene	
entF	Enterobactin synthesis	Yes	Yes	Yes
feoB	Ferrous iron transporter	No	Yes	
fepA	Ferri-enterobactin receptor	Yes	Yes	Yes
fepB	Enterobactin binding protein	Yes	Pseudogene	
fhuA	Ferrichrome receptor	Yes	Yes	
fhuE	Ferric-coprogen transporter	Yes	Pseudogene	
foxA	Ferrioxamine B transporter	Yes	Gene is absent	
iroBCDE	Salmochelin synthesis, export and utilization	Yes	Gene is absent	
iroN	Siderophore receptor	Yes	Gene is absent	Yes
iucABCD	Aerobactin synthesis	Gene is absent	Yes	
iutA	Aerobactin receptor	Gene is absent	Yes	
lysA	Lysine biosynthesis	No	Yes	
mgtA	Mg^{2+} transport ATPase	No	Yes	
mntH	Mn^{2+}/Fe^{2+} transport	Yes	Yes	
nrdHIEF	Ribonucleotide reductases	Yes	Yes	
phoRB	Regulation of pho regulon	No	Yes	

proVWX	Glycine, betaine, proline transport	No	Yes	
pstSC	Phosphate acquisition	No	Yes	
sfbABC	ABC-type transporter	Yes		
sitABCD	Mn^{2+}/Fe^{2+} transport	Yes	Yes	Yes
soxS	Regulation of superoxide response regulon	Yes	Yes	
sufA	Fe-S cluster maturation protein	Yes	Yes	Yes
uhpT	Sugar phosphate transporter	Yes	Yes	
yjjZ	Unknown function	Yes	Yes	

481 [a][80]; [b][81]; [c][91]; [d][82]; [e][83]
482

483 We identified twelve other signature genes of cytosolic colonization: *nrdHIEF*,
484 *sufABCDSE*, *yjjZ* and *uhpT* (Table 1). NrdEF is a Mn^{2+}-dependent ribonucleotide reductase that
485 functions under aerobic conditions, but only during iron restriction [94,95]. The *suf* operon
486 encodes for an iron-sulfur cluster system and is induced by oxidative stress and iron starvation
487 [96], like the *nrdHIEF* operon [97,98]. Fur is the master regulator of iron homeostasis in bacteria
488 [99]. While the function of YjjZ remains unknown, *yjjZ* (SL1344_4483) is part of the Fur regulon in
489 *S*. Typhimurium [100] and UPEC [101]. In summary, transcription of *nrdHIEF*, *sufABCDSE* and
490 *yjjZ* is controlled by iron deprivation and Fur. The sole metabolic gene identified as part of the
491 cytosol transcriptional signature is *uhpT*, a gene that is not induced by iron deprivation or oxidative
492 stress but rather by glucose-6-phosphate levels in the cytosol [80].

493 The combination of available transcriptome data revealed bacterial species-specific
494 cytosol-induced genes. Specifically, *bioA*, *lysA*, *pstSC*, *phoRB*, *proVWX* and *mgtA* were only
495 induced in *Shigella* and not in *S*. Typhimurium (Table 1; Dataset S1; [81,92]). The differential
496 expression profile suggests variance in the metabolic and phosphate acquisition strategies used
497 by these two pathogens in the epithelial cytosol. The contribution of Mg^{2+} transport also seems to
498 differ between the two bacteria, as *mgtA*-encoded Mg^{2+} acquisition is only induced by the cytosolic
499 environment for *S. flexneri*, and not for *S*. Typhimurium. Unlike *S. flexneri*, *S*. Typhimurium has a
500 second Mg^{2+} transport system encoded by *mgtB*, which is only up-regulated in the vacuole
501 (Dataset S1; Fig 5). *S. flexneri* does not encode for *mgtB*. Furthermore, the third Mg^{2+}/Ni^{2+}/Co^{2+}

502 transporter (CorA) is constitutively expressed in *S*. Typhimurium [102,103] and is required for
503 optimal proliferation in the cytosol [104]. The importance of Mn^{2+} acquisition also seems to differ
504 (see above).

505 We identified *S*. Typhimurium-specific genes/sRNAs that serve as signatures of the
506 cytosolic lifestyle. Examples include STnc3080, STnc3250, SL1802 and *siiABCDEF*, as well as
507 eight type III effectors that are translocated by T3SS1 (Fig 3, Fig 6, Figure S3, Dataset S1).
508 STnc3080, STnc3250 and SL1802 are all negatively regulated by Fur [32,100,105] and have not
509 previously been reported to play a role in *Salmonella* pathogenesis. Intracellular expression of
510 the *siiABCDEF* operon has not been reported before, prompting us to establish that the SiiE
511 protein, which mediates adhesion to the MUC1 on the apical surface of intestinal epithelial cells
512 [106], is both on the surface of cytosolic bacteria and secreted into the cytosol of epithelial cells
513 (Fig S5). The combination of findings from this study, and others [12,34], shows that cytosolic *S*.
514 Typhimurium are induced for T3SS1, secrete T3SS1-associated effectors, are flagellated and
515 decorated with SiiE. We conclude that cytosolic *S*. Typhimurium are "primed" to enter naïve
516 enterocytes following cellular release.

517 The major environmental factor that controls the transcriptional program of cytosol-
518 residing bacteria is clearly iron-limitation. Within mammalian cells, the "labile iron pool" refers to
519 the pool of chelatable and redox-active iron [107,108]. In resting cells, the labile iron pool is
520 estimated to be ~1 μM, representing only a minor fraction of the total cellular iron (50-100 μM)
521 [107,108]. At a subcellular level, measurements have shown that the concentration of labile iron
522 is lower in the cytosol than the nucleus, mitochondria or endosomes/lysosomes [109,110], in
523 agreement with our findings. We believe that consumption of free iron from the cytosol by rapidly
524 growing *S*. Typhimurium further depletes the pool compared to uninfected/resting cells.

525 The uniform induction of iron-responsive *S*. Typhimurium genes/sRNAs in the cytosol (Fig
526 3, Figure S3) indicates a generalized bacterial response to iron deprivation. Fur is the major iron-
527 responsive transcriptional regulator that controls iron homeostasis and oxidative stress defenses

528 in bacteria [99]. When bound to iron (i.e. in iron-replete conditions), Fur acts as both a repressor
529 and activator of gene expression, either directly or indirectly, and modulates expression of ~10%
530 of the *S*. Typhimurium genome [100,111]. Except for SL3990, all the low Fe^{2+}/bile shock-regulated
531 "up cytosol" genes/sRNAs (Dataset S1) that were validated using transcriptional reporters (Fig 3,
532 Fig S3) are negatively regulated by Fur [89,100,112](Fig 2). Many have a Fur box in their promoter
533 regions, the regulatory site to which iron-bound Fur binds, suggesting direct regulation. However,
534 an unanswered question is why all Fur-repressed *S*. Typhimurium genes/sRNAs are not induced
535 in the cytosolic population ([100]; Dataset S1). It is also unclear why SPI1-associated genes are
536 induced in a subset of cytosol-exposed bacteria in an iron-limited environment, when expression
537 of the SPI1 regulon is typically activated by iron-bound Fur under iron-replete conditions via HilD
538 and H-NS [113,114]. The regulation of SPI1 and its associated genes is complex [45], with
539 numerous environmental signals feeding into the regulatory network including osmolarity, oxygen
540 and bacterial growth phase, as well as iron. Bacterial cell-to-cell variation in the integration of all
541 the relevant signals could explain the phenotypic heterogeneity observed for SPI1-associated
542 gene expression in cytosolic bacteria. Such heterogeneity in T3SS1 gene expression has been
543 reported previously in broth cultures [115,116].

544 We have identified the site-specific cues encountered by *S*. Typhimurium in the distinct
545 milieus of a vacuole versus the cytosol. *S*. Typhimurium residing within the epithelial cytosol have
546 limited access to iron and manganese, are experiencing oxidative stress and utilize hexose-6-
547 phosphate sugars as a carbon source. Other studies of *S. flexneri* and *L. monocytogenes*
548 colonization suggested that the mammalian cytosol is a nutrient-rich environment of neutral pH
549 with low concentrations of Na^{2+}, Mg^{2+}, Ca^{2+} and PO_4^{3-} ions, but a high concentration of K^+
550 [79,81,117,118]. In contrast, the mature SCV is acidic [7,119,120], has high levels of K^+, Fe^{2+} and
551 oxygen, but is limiting in Mg^{2+}, PO_4^{3-} and Fe^{3+}, and *S*. Typhimurium are experiencing oxidative
552 stress but not amino acid starvation [40,41,81].

553 Based on single-cell analysis, we can refine previous conclusions drawn from population-
554 based studies of *S*. Typhimurium and epithelial cells. For example, in the landmark study of
555 Hautefort *et al*. (2008) [31], the simultaneous induction of SPI1 and flagella within epithelial cells
556 was reported, which at the time was puzzling. Single-cell microscopic analysis has solved this
557 mystery by showing that the cytosolic population is solely responsible for the intracellular
558 expression of both SPI1 and flagella ([12,14,34]; this study). Based on the intracellular induction
559 of *iroA*- and *mgtB*-*lacZ* reporter fusions in MDCK (epithelial) cells, concentrations of Fe^{2+} and Mg^{2+}
560 were thought to be low in the mature vacuole [121]. Additionally, a recent proteomic analysis of
561 *S*. Typhimurium isolated from infected epithelial cells at 6 h p.i. suggested that bacteria are
562 starved for numerous metals, including iron, manganese, and zinc [122]. Our findings show that
563 metal limitation experienced by intracellular bacteria is niche-dependent; levels of iron and
564 manganese are low in the cytosol, whereas zinc and magnesium are limiting in the vacuole.
565 Here, we demonstrate the importance of verifying results derived from population-based
566 studies at the single-cell level. We suggest that the many studies that have identified individual *S*.
567 Typhimurium or mammalian genes that influence bacterial proliferation in epithelial cells should
568 be revisited, especially if the distinct replication niches were not considered. As heterogeneity in
569 terms of bacterial proliferation and intracellular colonization site clearly influences the outcome of
570 infection [123,124], it is crucial that the study of host-pathogen interactions incorporates the
571 investigation of individual bacteria, as well as host cells.
572

573 **Materials and Methods**

574 **Bacterial strains and plasmids**

575 *S*. Typhimurium SL1344 was the wild-type strain used in this study [125]. Gene deletion mutants
576 were constructed using *sacB* allelic exchange, λ red recombinase technology or P22
577 transduction. SL1344 Δ*sitA* (deleted for amino acids 4-298), Δ*mntH* (deleted for amino acids 1-
578 411), Δ*yjjZ* (ΔSL1344_4483, deleted for amino acids 4-Fig 66) and ΔSL1344_1802 (deleted for
579 amino acids 4-53) deletion mutants were made via *sacB* negative selection. Two fragments of ~1
580 kb upstream and downstream of the gene of interest were amplified from *S*. Typhimurium SL1344
581 genomic DNA using Phusion High-Fidelity DNA polymerase (Thermo Scientific) (primer
582 sequences are listed in Table S1). The two fragments were combined for a second round of
583 amplification by overlap extension PCR. The amplicon was then digested with appropriate
584 restriction enzymes, ligated into the suicide vector pRE112 (Cm^R) [126], and electroporated into
585 *E. coli* SY327λpir. After sequence confirmation, the pRE112 plasmids were transferred to *E. coli*
586 SM10λpir (Kan^R) for conjugation into SL1344 wild-type or Δ*mntH* bacteria (for the Δ*sitA*Δ*mntH*
587 double mutant). For the second recombination event, *sacB*-based counterselection on LB agar
588 containing 5% (w/v) sucrose was used, and streptomycin-resistant, chloramphenicol-sensitive
589 colonies were screened by PCR with primers outside the recombination region to confirm the
590 deletion of each gene. *S*. Typhimurium SL1344 Δ*sufABCDSE*::kan, Δ*nrdHIEF*::kan, Δ*fhuB*::kan
591 and Δ*fepB*::kan strains were generated using λ red recombineering technology [127]. λ red
592 cassettes were amplified using pKD4 as a template with the oligonucleotide pairs listed in Table
593 S1 and electroporated into *S*. Typhimurium SL1344 wild-type containing the temperature-
594 sensitive helper plasmid, pKD46. Transformants were selected on LB agar plates containing
595 streptomycin (100 μg/ml) and kanamycin (50 μg/ml). Verification of λ red promoted gene
596 replacement was by PCR using a target-flanked primer and a kanamycin resistance gene-specific
597 primer. Each mutation was transferred into a clean SL1344 wild-type background using P22

598 phage transduction. The following insertional mutants were constructed by P22 transduction into
599 a SL1344 wild-type background from phage lysates prepared from the following *S*. Typhimurium
600 mutants: Δ*entC*::kan (Raffatellu, unpublished), Δ*iroN*::kan [84], ΔSTnc3080::kan (Kroeger,
601 unpublished), ΔSL1344_3990::kan [128], Δ*cysP*::kan [128], Δ*foxA*::kan [128], Δ*soxS*::kan [128],
602 Δ*sfbA*::kan [128], Δ*uhpT*::kan [128], Δ*lpxR*::kan [128], Δ*siiABCD*::kan [129]. Selection was on LB
603 agar plates containing kanamycin (50 µg/ml).

604 SL1344 wild-type bacteria constitutively expressing *mCherry* from the chromosome
605 (*glmS*::*Ptrc-mCherryST*::FRT, denoted as mCherry-*S*. Typhimurium) or a plasmid (pFPV-
606 mCherry) have been described previously [7,130]. *mCherry* expression is driven by the
607 constitutive *trc* promoter or *S*. Typhimurium *rpsM* promoter, respectively. The *PuhpT-gfpova*
608 plasmid, pNF101 [22], was used as a biosensor for bacterial exposure to the mammalian cytosol.
609 Expression of the unstable GFP variant, *gfp_ova* (protein half-life <60 min, [131]), is under the
610 control of the glucose-6-phosphate responsive *uhpT* promoter from *S. flexneri*. Alternatively,
611 bacterial access to the cytosol was assessed using the bidirectional reporter plasmid, pCHAR-
612 Duo(ASV), whereby constitutive *mCherry* expression is driven by the synthetic ProB promoter
613 and *gfpmut3.1(ASV)* expression is under the control of the *S*. Typhimurium *uhpT* promoter. To
614 create pCHAR-Duo(ASV), the coding sequence for the stable GFP variant, *gfpmut3.1* (protein
615 half-life >24 h), was excised from pCHAR-Duo [30] by XmaI/ApaI digestion and replaced with the
616 coding sequence for a destabilized GFP variant, *gfpmut3.1(ASV)* (protein half-life ~110 min),
617 which had been released from pGFP(ASV) (Clontech) by XmaI/ApaI digestion.

618 To construct fluorescent transcriptional reporters, we extracted the precise transcriptional
619 start sites from the online SalComMac database (http://tinyurl.com/SalComMac; [32,41]).
620 Approximately 500 bp of sequence upstream of the ATG start codon of each gene, or transcript
621 start site of each sRNA, was amplified from SL1344 genomic DNA with the oligonucleotide pairs
622 listed in Table S2. Amplicons were digested with XbaI/SmaI and ligated into the corresponding
623 restriction sites of pGFPmut3.1 (Clontech). XbaI/ApaI digestion released the gene/sRNA

624 promoter-*gfpmut3* fragment, which was then ligated into the corresponding sites of the low copy
625 number plasmid, pMPMA3ΔPlac [132]. The *pipB* and *sopB* promoters were excised from
626 pMPMA3ΔPlac-P*pipB*-GFP(LVA) and pMPMA3ΔPlac-P*sopB*-GFP(LVA), respectively [132], by
627 digestion with XbaI/KpnI and ligated into the corresponding sites of pGFPmut3.1 and then
628 transferred to pMPMA3ΔPlac as described above. The pMPMA3ΔPlac-P*uhpT-gfpmut3* construct
629 has been described previously [133]. GFP reporter plasmids were electroporated into wild-type
630 mCherry-*S*. Typhimurium.
631
632 **Reporter assays for metal sensitivity**
633 For metal repression studies, wild-type mCherry-*S*. Typhimurium bacteria harboring *gfpmut3*
634 fusions were grown shaking overnight (220 rpm) at 37°C in LB-Miller broth containing 100 µg/ml
635 streptomycin and 50 µg/ml carbenicillin, then washed twice in M9 salts pH 7.0 (6 g Na_2HPO_4, 3 g
636 KH_2PO_4, 0.5 g NaCl, 1 g NH_4Cl per liter) supplemented with 1 mM $MgSO_4$, 0.4% (w/v) glucose
637 and 0.01% (w/v) histidine – hereafter referred to as M9-supplemented media – and resuspended
638 in an equal volume of M9-supplemented media. Washed bacteria were diluted 1:200 in M9-
639 supplemented media containing 100 µg/ml streptomycin and 50 µg/ml carbenicillin and the
640 desired concentration of cobalt (II) chloride (Alfa Aesar, Puratronic®, 99.998%), iron (III) chloride
641 (Acros Organics, 99+%), manganese (II) chloride (Alfa Aesar, Puratronic®, 99.999%), nickel (II)
642 chloride (Alfa Aesar, Puratronic®, 99.9995%) or zinc chloride (Alfa Aesar, Puratronic®, 99.999%).
643 All solutions were prepared fresh in MilliQ water. Bacteria were grown overnight at 37°C, shaking
644 at 220 rpm for ~16 h. GFP fluorescence was measured in black 96-well plates (Costar) using a
645 TECAN SPARK plate reader (excitation wavelength of 485 nm, bandwidth 20 nm; emission
646 wavelength of 535 nm, bandwidth of 20 nm). All readings were normalized for bacterial growth
647 (OD_{600}). The background fluorescence of mCherry-*S*. Typhimurium bacteria (no reporter plasmid)
648 was subtracted from all readings.
649

650 **Mammalian cell culture**

651 HeLa human cervical adenocarcinoma epithelial cells were purchased from American Type
652 Culture Collection (ATCC, CCL-2) and used within 15 passages of receipt. Cells were maintained
653 at 37°C and 5% CO_2 in the growth medium (GM) recommended by ATCC i.e. Eagle's minimum
654 essential medium (EMEM, Corning) containing sodium pyruvate, L-glutamine and 10% (v/v) heat-
655 inactivated fetal calf serum (FCS; Gemini Bio Products). Tissue culture plasticware was
656 purchased from Thermo Scientific Nunc.

657

658 **Bacterial infection of mammalian cells**

659 HeLa cells were seeded 24 h prior to infection at the following densities: (i) $5x10^4$ cells/well in 24-
660 well tissue culture plates, (ii) $6x10^4$ cells/well on acid-washed glass coverslips in 24-well plates,
661 or (ii) $2.6x10^6$ cells/15 cm tissue culture dish. T3SS1-induced bacterial subcultures were prepared
662 in LB-Miller broth (Difco) [134] and cells were infected for 10 min with bacterial subcultures (MOI
663 ~50) as described [134]. To induce autophagy, HeLa cells were shifted to Earle's Balanced Salt
664 Solution (EBSS, Sigma) 3 h prior to infection and maintained in EBSS until 90 min post-infection.
665 Thereafter, infected cells were switched back to regular growth medium. To inhibit autophagy,
666 cells were incubated in growth media containing 100 nM wortmannin (WTM, Calbiochem) for 45
667 min prior to infection, continuing to 90 min post-infection, whereupon cells were transferred back
668 to regular growth media. For manipulation of cellular cation levels, epithelial cells were treated
669 16-18 h prior to infection in growth media containing 200 μM 2,2'-dipyridyl (DPI, Sigma-Aldrich),
670 200 μM DPI and 200 μM ammonium iron (III) citrate (FAC, Alfa Aesar) or 200 μM FAC alone. DPI
671 +/- FAC treatment continued throughout the infection. DPI was prepared as a 100 mM stock in
672 ethanol and stored at -80°C for a maximum of 2 weeks. FAC was prepared extemporaneously in
673 MilliQ water. Gentamicin protection and CHQ resistance assays (chloroquine diphosphate salt,
674 Sigma) were as described previously [134]. Monolayers were solubilized with 0.2% (w/v) sodium

675 deoxycholate (Sigma) and serial dilutions were plated on LB-Miller agar (Remel) for enumeration
676 of colony forming units (CFUs).
677
678 **Bacterial enrichment and RNA extraction from infected cells**
679 *S*. Typhimurium was enriched from infected HeLa cells (12 x 15 cm dishes for EBSS treatment,
680 6 x 15 cm dishes for WTM treatment) as described previously by Hautefort *et al*. (2008) [31] with
681 minor modifications. Briefly, infected HeLa cells were washed once with 30 ml chilled phosphate-
682 buffered saline (PBS), then lysed on ice for 10-20 min in 0.1% SDS, 1% acidic phenol, 19%
683 ethanol in water (15 ml per 15 cm dish). Pooled lysates were collected into 50 ml conical tubes
684 and centrifuged at 3,220 xg for 30 min, 4°C. After three washes in ice-cold wash buffer (0.1%
685 phenol, 19% ethanol in water) (30 min, 3,220 xg, 4°C each wash), the remaining bacterial pellet
686 was resuspended in <1 ml of wash buffer, transferred to an RNase-free microcentrifuge tube and
687 centrifuged at 16,000 xg for 2 min. The supernatant was discarded, and the pellet resuspended
688 in 1 ml TRIzol® reagent (Life Technologies) by gently pipetting up-and-down (~60 times), then
689 transferred to -80°C for storage. Total RNA was extracted as described [32] and the RNA
690 concentration quantified using a Nanodrop 2000 spectrophotometer (Thermo Scientific). RNA
691 quality was analyzed using an Agilent Bioanalyzer 2100. RNA samples isolated from two
692 independent experiments were sent to Vertis Biotechnologie AG (https://www.vertis-biotech.com)
693 for RNA sequencing.
694
695 **RNA-seq data analysis**
696 A total of 42 to 57 million sequence reads were generated from each sample on the Illumina HiSeq
697 platform. For the RankProduct analysis, segemehl [135] was used to map against the reference
698 genome sequence, resulting in 18.2 million uniquely mapped reads per sample on average. For
699 the BitSeq analysis, mapping against the transcriptome was required. This was accomplished
700 through Bowtie2 [136] and generated 7.1 million uniquely mapped reads per sample on average.

701 Gene/sRNA expression values were calculated by the Transcripts Per Million (TPM) approach
702 [137]. All genes/sRNAs with mapped reads were reported as TPM and a threshold TPM value of
703 10 was used as a cut-off to distinguish gene expression from background noise [32].
704 Genes/sRNAs were deemed differentially expressed using fold-change criteria of ≥1.40 (cytosol
705 up-regulated) and ≤0.71 (vacuole up-regulated) for WTM/EBSS treatment conditions (cells
706 highlighted in yellow in Dataset S1). Statistical significance was assessed using two independent
707 platforms, Bayesian interference of transcripts from sequencing data (BitSeq; [138]) and rank
708 products (RankProduct; [139,140]). For Bitseq analysis, we arbitrarily set a Probability of Positive
709 Log Ratio (PPLR) of ≥0.90 for "up cytosol" genes/sRNAs and ≤0.1 for "up vacuole" genes/sRNAs
710 for statistical significance (cells highlighted in green in Dataset S1). For RankProduct analysis,
711 the cutoff for differentially expressed genes was arbitrarily set to a percentage of false positive
712 (pfp) value of ≤0.2 (cells highlighted in green in Dataset S1) for statistical significance.
713

714 **Pathway enrichment analysis**

715 A collection of 80 custom pathways was generated from previous RNA-seq, ChIP-seq, and
716 microarray studies of *S.* Typhimurium regulons [100,111,114,141,142], as well as transcriptional
717 profiling of *S.* Typhimurium 4/74 under infection-relevant *in vitro* growth conditions [32] and inside
718 murine macrophages [41]. Detailed description of the pathway curation process and all relevant
719 scripts can be found at https://github.com/apredeus/salmonella_pathways. Additionally, KEGG
720 pathways for *S*. Typhimurium SL1344 were obtained using the KEGGREST R package v1.28.0,
721 and gene ontology (GO) mapping of SL1344 genes was extracted from SL1344 protein annotation
722 by InterProScan v5.41-78. See Dataset S2 for the entire dataset. The combined pathways were
723 used to annotate gene sets up-regulated in the vacuole and cytosol using the clusterProfiler R
724 package v3.16.1. The resulting overlaps were visualized using ggplot2 v3.3.2.
725

726 **Fluorescence microscopy**

727 HeLa cells were seeded on acid-washed, 12 mm glass coverslips (#1.5 thickness, Fisher
728 Scientific) in 24-well plates. Infected HeLa cells were fixed with 2.5% (w/v) paraformaldehyde in
729 PBS for 10 min at 37°C. The immunostaining procedure has been described previously [22].
730 Rabbit anti-SiiE serum (kindly provided by Michael Hensel) was used at a dilution of 1:200.
731 Digitonin permeabilization to deliver anti-*Salmonella* LPS antibodies (*Salmonella* O-Antiserum
732 Group B Factors 1, 4, 5, 12; Difco; 1:300 dilution) directly to the cytosol was as described
733 previously [14]. Cells were stained with Hoechst 33342 (1:10,000 in DDH_2O, Life Technologies)
734 to label DNA and coverslips were mounted onto glass slides using Mowiol. Samples were
735 visualized on a Leica DM4000 upright fluorescence microscope for scoring the number of bacteria
736 per cell, the proportion of cytosolic bacteria and quantification of transcriptional reporter activity.
737 ImageJ software was used to quantify the activity of transcriptional reporters at the individual
738 bacterium level. Images in the red (mCherry) and green (GFP) channels were acquired under 63x
739 magnification on a Leica DM4000 upright fluorescent microscope using the same acquisition
740 settings (exposure and gain) for each group of transcriptional reporters (determined by the
741 reporter with the highest intensity in the green fluorescence channel). A minimum of 100 cytosolic
742 and 100 vacuolar bacteria, from cells with ≥100 bacteria and 2-40 bacteria, respectively, acquired
743 from ≥5 fields of view were quantified for each transcriptional reporter from each experiment. From
744 grayscale images, well-defined, individual bacteria were randomly chosen on the mCherry
745 channel (represents all bacteria) and manually outlined, converted to a binary image and the pixel
746 intensity associated with each identified particle (i.e. one bacterium) quantified from the
747 corresponding GFP channel image. GFP fluorescence/bacterium was subsequently plotted as
748 the mean fluorescence intensity (MFI).
749 Image acquisition on a Leica SP8 Scanning Point confocal microscope was using the
750 sequential acquisition mode through an optical section of 0.3 μm in the z-axis. Images are
751 maximum intensity projections of z-stacks.
752

753 **Statistical analysis**

754 All experiments were conducted on at least three separate occasions, unless otherwise indicated,
755 and results are presented as mean ± SD. Except for the RNA-seq data (see separate paragraph
756 on RNA-seq data analysis), statistical analyses were performed using one-way analysis of
757 variance (ANOVA) with Dunnett's post-hoc test or Student's t-test (GraphPad Prism). A p-value
758 of ≤0.05 was considered significant.

759 **Acknowledgements**

760 We kindly thank Michael McClelland, Corrie Detweiler, Carsten Kroeger, Denise Monack, Martina
761 Sassone-Corsi and Manuela Raffatellu for sharing bacterial mutants; Michael Hensel for providing
762 the anti-SiiE antibody; Olivia Steele-Mortimer for providing the pCHAR-Duo plasmid; Zeus
763 Saldana-Ahuactzi and Sadie Izaguirre for generating the P*zinT-gfpmut3* and P*mgtC-gfpmut3*
764 constructs; Isabelle Hautefort for invaluable advice about bacterial RNA purification; Andrea
765 Battistoni for helpful discussions about zinc transporters and Jean Celli and Johanna Elfenbein
766 for critical reading of this manuscript.

767

768 **References**

769 1. Fredlund J, Enninga J. Cytoplasmic access by intracellular bacterial pathogens. Trends in
770 Microbiology. 2014;22: 128–137. doi:10.1016/j.tim.2014.01.003

771 2. Knodler LA. Salmonella enterica: living a double life in epithelial cells. Current Opinion
772 in Microbiology. 2015;23: 23–31. doi:10.1016/j.mib.2014.10.010

773 3. Bierne H, Milohanic E, Kortebi M. To Be Cytosolic or Vacuolar: The Double Life of
774 Listeria monocytogenes. Front Cell Infect Microbiol. 2018;8: 136.
775 doi:10.3389/fcimb.2018.00136

776 4. Kirk MD, Pires SM, Black RE, Caipo M, Crump JA, Devleesschauwer B, et al. World
777 Health Organization Estimates of the Global and Regional Disease Burden of 22
778 Foodborne Bacterial, Protozoal, and Viral Diseases, 2010: A Data Synthesis. PLOS
779 Medicine. 2015;12: e1001921. doi:10.1371/journal.pmed.1001921

780 5. Stanaway JD, Parisi A, Sarkar K, Blacker BF, Reiner RC, Hay SI, et al. The global burden
781 of non-typhoidal salmonella invasive disease: a systematic analysis for the Global Burden
782 of Disease Study 2017. The Lancet Infectious Diseases. 2019;19: 1312–1324.
783 doi:10.1016/S1473-3099(19)30418-9

784 6. Steele-Mortimer O, Méresse S, Gorvel J-P, Toh B-H, Finlay BB. Biogenesis of
785 Salmonella typhimurium-containing vacuoles in epithelial cells involves interactions with
786 the early endocytic pathway. Cellular Microbiology. 1999;1: 33–49.
787 doi:https://doi.org/10.1046/j.1462-5822.1999.00003.x

788 7. Drecktrah D, Knodler LA, Howe D, Steele-Mortimer O. Salmonella trafficking is defined
789 by continuous dynamic interactions with the endolysosomal system. Traffic. 2007;8: 212–
790 225. doi:10.1111/j.1600-0854.2006.00529.x

791 8. Hume PJ, Singh V, Davidson AC, Koronakis V. Swiss Army Pathogen: The Salmonella
792 Entry Toolkit. Front Cell Infect Microbiol. 2017;7: 348. doi:10.3389/fcimb.2017.00348

793 9. Deiwick J, Nikolaus T, Erdogan S, Hensel M. Environmental regulation of Salmonella
794 pathogenicity island 2 gene expression. Mol Microbiol. 1999;31: 1759–1773.
795 doi:10.1046/j.1365-2958.1999.01312.x

796 10. Beuzón CR, Banks G, Deiwick J, Hensel M, Holden DW. pH-dependent secretion of
797 SseB, a product of the SPI-2 type III secretion system of Salmonella typhimurium.
798 Molecular Microbiology. 1999;33: 806–816. doi:10.1046/j.1365-2958.1999.01527.x

799 11. Castanheira S, García-del Portillo F. Salmonella Populations inside Host Cells. Front Cell
800 Infect Microbiol. 2017;7: 432. doi:10.3389/fcimb.2017.00432

801 12. Knodler LA, Vallance BA, Celli J, Winfree S, Hansen B, Montero M, et al. Dissemination
802 of invasive Salmonella via bacterial-induced extrusion of mucosal epithelia. Proc Natl
803 Acad Sci USA. 2010;107: 17733–17738. doi:10.1073/pnas.1006098107

804 13. Malik-Kale P, Winfree S, Steele-Mortimer O. The bimodal lifestyle of intracellular
805 Salmonella in epithelial cells: replication in the cytosol obscures defects in vacuolar
806 replication. PLoS ONE. 2012;7: e38732. doi:10.1371/journal.pone.0038732

807 14. Knodler LA, Nair V, Steele-Mortimer O. Quantitative assessment of cytosolic Salmonella
808 in epithelial cells. PLoS ONE. 2014;9: e84681. doi:10.1371/journal.pone.0084681

809 15. Fowler CC, Galán JE. Decoding a Salmonella Typhi Regulatory Network that Controls
810 Typhoid Toxin Expression within Human Cells. Cell Host & Microbe. 2018;23: 65-76.e6.
811 doi:10.1016/j.chom.2017.12.001

812 16. Hausmann A, Böck D, Geiser P, Berthold DL, Fattinger SA, Furter M, et al. Intestinal
813 epithelial NAIP/NLRC4 restricts systemic dissemination of the adapted pathogen
814 Salmonella Typhimurium due to site-specific bacterial PAMP expression. Mucosal
815 Immunol. 2020. doi:10.1038/s41385-019-0247-0

816 17. Laughlin RC, Knodler LA, Barhoumi R, Payne HR, Wu J, Gomez G, et al. Spatial
817 Segregation of Virulence Gene Expression during Acute Enteric Infection with Salmonella
818 enterica serovar Typhimurium. mBio. 2014;5. doi:10.1128/mBio.00946-13

819 18. Beuzón CR, Salcedo SP, Holden DW. Growth and killing of a Salmonella enterica serovar
820 Typhimurium sifA mutant strain in the cytosol of different host cell lines. Microbiology
821 (Reading, Engl). 2002;148: 2705–2715. doi:10.1099/00221287-148-9-2705

822 19. Thurston TLM, Matthews SA, Jennings E, Alix E, Shao F, Shenoy AR, et al. Growth
823 inhibition of cytosolic Salmonella by caspase-1 and caspase-11 precedes host cell death.
824 Nat Commun. 2016;7: 13292. doi:10.1038/ncomms13292

825 20. Kohler LJ, Roy CR. Autophagic targeting and avoidance in intracellular bacterial
826 infections. Current Opinion in Microbiology. 2017;35: 36–41.
827 doi:10.1016/j.mib.2016.11.004

828 21. Birmingham CL, Smith AC, Bakowski MA, Yoshimori T, Brumell JH. Autophagy
829 controls Salmonella infection in response to damage to the Salmonella-containing vacuole.
830 J Biol Chem. 2006;281: 11374–11383. doi:10.1074/jbc.M509157200

831 22. Lau N, Haeberle AL, O'Keeffe BJ, Latomanski EA, Celli J, Newton HJ, et al. SopF, a
832 phosphoinositide binding effector, promotes the stability of the nascent Salmonella-
833 containing vacuole. PLOS Pathogens. 2019;15: e1007959.
834 doi:10.1371/journal.ppat.1007959

835 23. Xu Y, Zhou P, Cheng S, Lu Q, Nowak K, Hopp A-K, et al. A Bacterial Effector Reveals
836 the V-ATPase-ATG16L1 Axis that Initiates Xenophagy. Cell. 2019;0.
837 doi:10.1016/j.cell.2019.06.007

838 24. Thurston TLM, Wandel MP, Muhlinen N von, Foeglein Á, Randow F. Galectin 8 targets
839 damaged vesicles for autophagy to defend cells against bacterial invasion. Nature.
840 2012;482: 414–418. doi:10.1038/nature10744

841 25. Ravenhill BJ, Boyle KB, von Muhlinen N, Ellison CJ, Masson GR, Otten EG, et al. The
842 Cargo Receptor NDP52 Initiates Selective Autophagy by Recruiting the ULK Complex to
843 Cytosol-Invading Bacteria. Mol Cell. 2019;74: 320-329.e6.
844 doi:10.1016/j.molcel.2019.01.041

845 26. Kreibich S, Emmenlauer M, Fredlund J, Rämö P, Münz C, Dehio C, et al. Autophagy
846 Proteins Promote Repair of Endosomal Membranes Damaged by the Salmonella Type
847 Three Secretion System 1. Cell Host & Microbe. 2015;18: 527–537.
848 doi:10.1016/j.chom.2015.10.015

849 27. Yu HB, Croxen MA, Marchiando AM, Ferreira RBR, Cadwell K, Foster LJ, et al.
850 Autophagy facilitates Salmonella replication in HeLa cells. MBio. 2014;5: e00865-00814.
851 doi:10.1128/mBio.00865-14

852 28. Klionsky DJ, Abdelmohsen K, Abe A, Abedin MJ, Abeliovich H, Acevedo Arozena A, et
853 al. Guidelines for the use and interpretation of assays for monitoring autophagy (3rd
854 edition). Autophagy. 2016;12: 1–222. doi:10.1080/15548627.2015.1100356

855 29. Brumell JH, Tang P, Zaharik ML, Finlay BB. Disruption of the Salmonella-Containing
856 Vacuole Leads to Increased Replication of Salmonella enterica Serovar Typhimurium in
857 the Cytosol of Epithelial Cells. IAI. 2002;70: 3264–3270. doi:10.1128/IAI.70.6.3264-
858 3270.2002

859 30. Chong A, Starr T, Finn CE, Steele-Mortimer O. A role for the Salmonella Type III
860 Secretion System 1 in bacterial adaptation to the cytosol of epithelial cells. Molecular
861 Microbiology. 2019;112: 1270–1283. doi:10.1111/mmi.14361

862 31. Hautefort I, Thompson A, Eriksson-Ygberg S, Parker ML, Lucchini S, Danino V, et al.
863 During infection of epithelial cells Salmonella enterica serovar Typhimurium undergoes a
864 time-dependent transcriptional adaptation that results in simultaneous expression of three
865 type 3 secretion systems. Cellular Microbiology. 2008;10: 958–984. doi:10.1111/j.1462-
866 5822.2007.01099.x

867 32. Kröger C, Colgan A, Srikumar S, Händler K, Sivasankaran SK, Hammarlöf DL, et al. An
868 Infection-Relevant Transcriptomic Compendium for Salmonella enterica Serovar
869 Typhimurium. Cell Host & Microbe. 2013;14: 683–695. doi:10.1016/j.chom.2013.11.010

870 33. Kröger C, Dillon SC, Cameron ADS, Papenfort K, Sivasankaran SK, Hokamp K, et al.
871 The transcriptional landscape and small RNAs of Salmonella enterica serovar
872 Typhimurium. PNAS. 2012;109: E1277–E1286. doi:10.1073/pnas.1201061109

873 34. Finn CE, Chong A, Cooper KG, Starr T, Steele-Mortimer O. A second wave of
874 Salmonella T3SS1 activity prolongs the lifespan of infected epithelial cells. PLoS Pathog.
875 2017;13: e1006354. doi:10.1371/journal.ppat.1006354

876 35. Gerlach RG, Jäckel D, Geymeier N, Hensel M. Salmonella Pathogenicity Island 4-
877 Mediated Adhesion Is Coregulated with Invasion Genes in Salmonella enterica. IAI.
878 2007;75: 4697–4709. doi:10.1128/IAI.00228-07

879 36. Main-Hester KL, Colpitts KM, Thomas GA, Fang FC, Libby SJ. Coordinate Regulation of
880 Salmonella Pathogenicity Island 1 (SPI1) and SPI4 in Salmonella enterica Serovar
881 Typhimurium. IAI. 2008;76: 1024–1035. doi:10.1128/IAI.01224-07

882 37. Galyov EE, Wood MW, Rosqvist R, Mullan PB, Watson PR, Hedges S, et al. A secreted
883 effector protein of Salmonella dublin is translocated into eukaryotic cells and mediates
884 inflammation and fluid secretion in infected ileal mucosa. Molecular Microbiology.
885 1997;25: 903–912. doi:https://doi.org/10.1111/j.1365-2958.1997.mmi525.x

886 38. Zhou D, Chen L-M, Hernandez L, Shears SB, Galán JE. A Salmonella inositol
887 polyphosphatase acts in conjunction with other bacterial effectors to promote host cell
888 actin cytoskeleton rearrangements and bacterial internalization. Molecular Microbiology.
889 2001;39: 248–260. doi:10.1046/j.1365-2958.2001.02230.x

890 39. Cheng S, Wang L, Liu Q, Qi L, Yu K, Wang Z, et al. Identification of a Novel Salmonella
891 Type III Effector by Quantitative Secretome Profiling. Mol Cell Proteomics. 2017;16:
892 2219–2228. doi:10.1074/mcp.RA117.000230

893 40. Eriksson S, Lucchini S, Thompson A, Rhen M, Hinton JCD. Unravelling the biology of
894 macrophage infection by gene expression profiling of intracellular Salmonella enterica.
895 Molecular Microbiology. 2003;47: 103–118. doi:https://doi.org/10.1046/j.1365-
896 2958.2003.03313.x

897 41. Srikumar S, Kröger C, Hébrard M, Colgan A, Owen SV, Sivasankaran SK, et al. RNA-seq
898 Brings New Insights to the Intra-Macrophage Transcriptome of Salmonella Typhimurium.
899 PLOS Pathogens. 2015;11: e1005262. doi:10.1371/journal.ppat.1005262

900 42. Gunn JS, Alpuche-Aranda CM, Loomis WP, Belden WJ, Miller SI. Characterization of the
901 Salmonella typhimurium pagC/pagD chromosomal region. Journal of bacteriology.
902 1995;177: 5040–5047. doi:10.1128/JB.177.17.5040-5047.1995

903 43. Blondel CJ, Jiménez JC, Contreras I, Santiviago CA. Comparative genomic analysis
904 uncovers 3 novel loci encoding type six secretion systems differentially distributed in
905 Salmonella serotypes. BMC Genomics. 2009;10: 354. doi:10.1186/1471-2164-10-354

906 44. Sabbagh SC, Forest CG, Lepage C, Leclerc J-M, Daigle F. So similar, yet so different:
907 uncovering distinctive features in the genomes of Salmonella enterica serovars
908 Typhimurium and Typhi: Genomic comparison of S. Typhimurium and S. Typhi. FEMS
909 Microbiology Letters. 2010;305: 1–13. doi:10.1111/j.1574-6968.2010.01904.x

910 45. Ellermeier JR, Slauch JM. Adaptation to the host environment: regulation of the SPI1 type
911 III secretion system in Salmonella enterica serovar Typhimurium. Current Opinion in
912 Microbiology. 2007;10: 24–29. doi:10.1016/j.mib.2006.12.002

913 46. Roche B, Bumann D. Single-cell reporters for pathogen responses to antimicrobial host
914 attacks. Current Opinion in Microbiology. 2021;59: 16–23. doi:10.1016/j.mib.2020.07.013

915 47. Bumann D, Valdivia RH. Identification of host-induced pathogen genes by differential
916 fluorescence induction reporter systems. Nat Protoc. 2007;2: 770–777.
917 doi:10.1038/nprot.2007.78

918 48. Valdivia RH, Falkow S. Fluorescence-Based Isolation of Bacterial Genes Expressed
919 Within Host Cells. Science. 1997;277: 2007–2011. doi:10.1126/science.277.5334.2007

920 49. Maguire ME. Magnesium, Manganese, and Divalent Cation Transport Assays in Intact
921 Cells. In: Schatten H, Eisenstark A, editors. Salmonella. Totowa, NJ: Humana Press;
922 2007. pp. 289–305. doi:10.1007/978-1-59745-512-1_14

923 50. Chambers JAA. CHAPTER 1 - BUFFERS, CHELATING AGENTS AND
924 DENATURANTS. In: Chambers JAA, Rickwood D, editors. Biochemistry Labfax.
925 Academic Press; 1993. pp. 1–36. doi:10.1016/B978-0-12-167340-6.50008-2

926 51. Ikeda JS, Janakiraman A, Kehres DG, Maguire ME, Slauch JM. Transcriptional
927 Regulation of sitABCD of Salmonella enterica Serovar Typhimurium by MntR and Fur.
928 JB. 2005;187: 912–922. doi:10.1128/JB.187.3.912-922.2005

929 52. Breuer W, Epsztejn S, Cabantchik ZI. Iron Acquired from Transferrin by K562 Cells Is
930 Delivered into a Cytoplasmic Pool of Chelatable Iron(II). J Biol Chem. 1995;270: 24209–
931 24215. doi:10.1074/jbc.270.41.24209

932 53. Nakamura K, Kawakami T, Yamamoto N, Tomizawa M, Fujiwara T, Ishii T, et al.
933 Activation of the NLRP3 inflammasome by cellular labile iron. Experimental
934 Hematology. 2016;44: 116–124. doi:10.1016/j.exphem.2015.11.002

935 54. Kehres DG, Janakiraman A, Slauch JM, Maguire ME. Regulation of Salmonella enterica
936 Serovar Typhimurium mntH Transcription by H2O2, Fe2+, and Mn2+. J BACTERIOL.
937 2002;184: 8.

938 55. Kim CC, Falkow S. Delineation of Upstream Signaling Events in the Salmonella
939 Pathogenicity Island 2 Transcriptional Activation Pathway. JB. 2004;186: 4694–4704.
940 doi:10.1128/JB.186.14.4694-4704.2004

941 56. Osman D, Cavet JS. Chapter 5 - Metal Sensing in Salmonella: Implications for
942 Pathogenesis. In: Poole RK, editor. Advances in Microbial Physiology. Academic Press;
943 2011. pp. 175–232. doi:10.1016/B978-0-12-381043-4.00005-2

944 57. Kehres DG, Zaharik ML, Finlay BB, Maguire ME. The NRAMP proteins of Salmonella
945 typhimurium and Escherichia coli are selective manganese transporters involved in the
946 response to reactive oxygen. Molecular Microbiology. 2000;36: 1085–1100.
947 doi:10.1046/j.1365-2958.2000.01922.x

948 58. Kehres DG, Janakiraman A, Slauch JM, Maguire ME. SitABCD Is the Alkaline Mn2+
949 Transporter of Salmonella enterica Serovar Typhimurium. J BACTERIOL. 2002;184: 8.

950 59. Ammendola S, Pasquali P, Pistoia C, Petrucci P, Petrarca P, Rotilio G, et al. High-Affinity
951 Zn2+ Uptake System ZnuABC Is Required for Bacterial Zinc Homeostasis in Intracellular
952 Environments and Contributes to the Virulence of Salmonella enterica. IAI. 2007;75:
953 5867–5876. doi:10.1128/IAI.00559-07

954 60. Petrarca P, Ammendola S, Pasquali P, Battistoni A. The Zur-Regulated ZinT Protein Is an
955 Auxiliary Component of the High-Affinity ZnuABC Zinc Transporter That Facilitates
956 Metal Recruitment during Severe Zinc Shortage. JB. 2010;192: 1553–1564.
957 doi:10.1128/JB.01310-09

958 61. Ilari A, Alaleona F, Tria G, Petrarca P, Battistoni A, Zamparelli C, et al. The Salmonella
959 enterica ZinT structure, zinc affinity and interaction with the high-affinity uptake protein
960 ZnuA provide insight into the management of periplasmic zinc. Biochimica et Biophysica
961 Acta (BBA) - General Subjects. 2014;1840: 535–544. doi:10.1016/j.bbagen.2013.10.010

962 62. Grass G, Franke S, Taudte N, Nies DH, Kucharski LM, Maguire ME, et al. The Metal
963 Permease ZupT from Escherichia coli Is a Transporter with a Broad Substrate Spectrum.
964 JB. 2005;187: 1604–1611. doi:10.1128/JB.187.5.1604-1611.2005

965 63. Karlinsey JE, Maguire ME, Becker LA, Crouch M-LV, Fang FC. The phage shock protein
966 PspA facilitates divalent metal transport and is required for virulence of Salmonella
967 enterica sv. Typhimurium. Molecular Microbiology. 2010;78: 669–685.
968 doi:10.1111/j.1365-2958.2010.07357.x

969 64. Cerasi M, Ammendola S, Battistoni A. Competition for zinc binding in the host-pathogen
970 interaction. Front Cell Infect Microbiol. 2013;3. doi:10.3389/fcimb.2013.00108

971 65. Groisman EA, Hollands K, Kriner MA, Lee E-J, Park S-Y, Pontes MH. Bacterial Mg2+
972 Homeostasis, Transport, and Virulence. Annu Rev Genet. 2013;47: 625–646.
973 doi:10.1146/annurev-genet-051313-051025

974 66. Smith RL, Kaczmarek MT, Kucharski LM, Maguire ME. Magnesium transport in
975 Samonella typhimurium :regulation of mgtA and mgtC during invasion of epithelial and
976 macrophage cells. 1998; 9.

977 67. Knodler LA, Celli J, Hardt W-D, Vallance BA, Yip C, Finlay BB. Salmonella effectors
978 within a single pathogenicity island are differentially expressed and translocated by
979 separate type III secretion systems. Molecular Microbiology. 2002;43: 1089–1103.
980 doi:10.1046/j.1365-2958.2002.02820.x

981 68. Morgan E, Bowen AJ, Carnell SC, Wallis TS, Stevens MP. SiiE Is Secreted by the
982 Salmonella enterica Serovar Typhimurium Pathogenicity Island 4-Encoded Secretion
983 System and Contributes to Intestinal Colonization in Cattle. IAI. 2007;75: 1524–1533.
984 doi:10.1128/IAI.01438-06

985 69. Gerlach RG, Jäckel D, Stecher B, Wagner C, Lupas A, Hardt W-D, et al. Salmonella
986 Pathogenicity Island 4 encodes a giant non-fimbrial adhesin and the cognate type 1

987 secretion system. Cellular Microbiology. 2007;9: 1834–1850. doi:10.1111/j.1462-
988 5822.2007.00919.x

989 70. Martínez-Flores I, Pérez-Morales D, Sánchez-Pérez M, Paredes CC, Collado-Vides J,
990 Salgado H, et al. In silico clustering of Salmonella global gene expression data reveals
991 novel genes co-regulated with the SPI-1 virulence genes through HilD. Scientific Reports.
992 2016;6: 37858. doi:10.1038/srep37858

993 71. Karlinsey JE, Bang I-S, Becker LA, Frawley ER, Porwollik S, Robbins HF, et al. The
994 NsrR regulon in nitrosative stress resistance of Salmonella enterica serovar Typhimurium.
995 Molecular Microbiology. 2012;85: 1179–1193. doi:https://doi.org/10.1111/j.1365-
996 2958.2012.08167.x

997 72. Felton J, Michaelis S, Wright A. Mutations in two unlinked genes are required to produce
998 asparagine auxotrophy in Escherichia coli. Journal of Bacteriology. 1980;142: 221–228.

999 73. Turnbull AL, Surette MG. L-Cysteine is required for induced antibiotic resistance in
1000 actively swarming Salmonella enterica serovar Typhimurium. Microbiology. 2008;154:
1001 3410–3419. doi:10.1099/mic.0.2008/020347-0

1002 74. Fang FC, Vazquez-Torres A, Xu Y. The transcriptional regulator SoxS is required for
1003 resistance of Salmonella typhimurium to paraquat but not for virulence in mice. Infection
1004 and Immunity. 1997;65: 5371–5375.

1005 75. Pomposiello PJ, Demple B. Identification of SoxS-Regulated Genes in Salmonella
1006 enterica Serovar Typhimurium. J Bacteriol. 2000;182: 23–29.

1007 76. Pattery T, Hernalsteens J-P, Greve HD. Identification and molecular characterization of a
1008 novel Salmonella enteritidis pathogenicity islet encoding an ABC transporter. Molecular
1009 Microbiology. 1999;33: 791–805. doi:10.1046/j.1365-2958.1999.01526.x

1010 77. Klein JA, Grenz JR, Slauch JM, Knodler LA. Controlled Activity of the Salmonella
1011 Invasion-Associated Injectisome Reveals Its Intracellular Role in the Cytosolic
1012 Population. MBio. 2017;8. doi:10.1128/mBio.01931-17

1013 78. Röder J, Hensel M. Presence of SopE and mode of infection result in increased
1014 Salmonella-containing vacuole damage and cytosolic release during host cell infection by
1015 Salmonella enterica. Cellular Microbiology. 2020;22: e13155.
1016 doi:https://doi.org/10.1111/cmi.13155

1017 79. Eisenreich W, Dandekar T, Heesemann J, Goebel W. Carbon metabolism of intracellular
1018 bacterial pathogens and possible links to virulence. Nature Reviews Microbiology. 2010;8:
1019 401–412. doi:10.1038/nrmicro2351

1020 80. Runyen-Janecky LJ, Payne SM. Identification of chromosomal Shigella flexneri genes
1021 induced by the eukaryotic intracellular environment. Infect Immun. 2002;70: 4379–4388.
1022 doi:10.1128/iai.70.8.4379-4388.2002

1023 81. Lucchini S, Liu H, Jin Q, Hinton JCD, Yu J. Transcriptional adaptation of Shigella
1024 flexneri during infection of macrophages and epithelial cells: insights into the strategies of
1025 a cytosolic bacterial pathogen. Infect Immun. 2005;73: 88–102. doi:10.1128/IAI.73.1.88-
1026 102.2005

1027 82. Reigstad CS, Hultgren SJ, Gordon JI. Functional Genomic Studies of Uropathogenic
1028 *Escherichia coli* and Host Urothelial Cells when Intracellular Bacterial Communities Are
1029 Assembled. J Biol Chem. 2007;282: 21259–21267. doi:10.1074/jbc.M611502200

1030 83. Conover MS, Hadjifrangiskou M, Palermo JJ, Hibbing ME, Dodson KW, Hultgren SJ.
1031 Metabolic Requirements of Escherichia coli in Intracellular Bacterial Communities during
1032 Urinary Tract Infection Pathogenesis. mBio. 2016;7: e00104-00116.
1033 doi:10.1128/mBio.00104-16

1034 84. Nagy TA, Moreland SM, Andrews-Polymenis H, Detweiler CS. The Ferric Enterobactin
1035 Transporter Fep Is Required for Persistent Salmonella enterica Serovar Typhimurium
1036 Infection. Payne SM, editor. Infect Immun. 2013;81: 4063–4070. doi:10.1128/IAI.00412-
1037 13

1038 85. Osman D, Martini MA, Foster AW, Chen J, Scott AJP, Morton RJ, et al. Bacterial sensors
1039 define intracellular free energies for correct enzyme metalation. Nat Chem Biol. 2019;15:
1040 241–249. doi:10.1038/s41589-018-0211-4

1041 86. Skare JT, Ahmer BM, Seachord CL, Darveau RP, Postle K. Energy transduction between
1042 membranes. TonB, a cytoplasmic membrane protein, can be chemically cross-linked in
1043 vivo to the outer membrane receptor FepA. J Biol Chem. 1993;268: 16302–16308.

1044 87. Hantke K, Nicholson G, Rabsch W, Winkelmann G. Salmochelins, siderophores of
1045 Salmonella enterica and uropathogenic Escherichia coli strains, are recognized by the
1046 outer membrane receptor IroN. Proceedings of the National Academy of Sciences.
1047 2003;100: 3677–3682. doi:10.1073/pnas.0737682100

1048 88. Rabsch W, Voigt W, Reissbrodt R, Tsolis RM, Bäumler AJ. Salmonella typhimurium
1049 IroN and FepA Proteins Mediate Uptake of Enterobactin but Differ in Their Specificity for
1050 Other Siderophores. J Bacteriol. 1999;181: 3610–3612. doi:10.1128/JB.181.11.3610-
1051 3612.1999

1052 89. Tsolis RM, Bäumler AJ, Stojiljkovic I, Heffron F. Fur regulon of Salmonella
1053 typhimurium: identification of new iron-regulated genes. Journal of bacteriology.
1054 1995;177: 4628–4637. doi:10.1128/JB.177.16.4628-4637.1995

1055 90. Payne SM, Wyckoff EE, Murphy ER, Oglesby AG, Boulette ML, Davies NML. Iron and
1056 Pathogenesis of Shigella: Iron Acquisition in the Intracellular Environment. Biometals.
1057 2006;19: 173–180. doi:10.1007/s10534-005-4577-x

1058 91. Runyen-Janecky L, Dazenski E, Hawkins S, Warner L. Role and Regulation of the
1059 Shigella flexneri Sit and MntH Systems. IAI. 2006;74: 4666–4672.
1060 doi:10.1128/IAI.00562-06

1061 92. Runyen-Janecky LJ, Reeves SA, Gonzales EG, Payne SM. Contribution of the Shigella
1062 flexneri Sit, Iuc, and Feo Iron Acquisition Systems to Iron Acquisition In Vitro and in
1063 Cultured Cells. Infection and Immunity. 2003;71: 1919–1928. doi:10.1128/IAI.71.4.1919-
1064 1928.2003

1065 93. Crouch M-LV, Castor M, Karlinsey JE, Kalhorn T, Fang FC. Biosynthesis and IroC-
1066 dependent export of the siderophore salmochelin are essential for virulence of Salmonella
1067 enterica serovar Typhimurium. Molecular Microbiology. 2008;67: 971–983.
1068 doi:10.1111/j.1365-2958.2007.06089.x

1069 94. Andrews SC. Making DNA without iron – induction of a manganese-dependent
1070 ribonucleotide reductase in response to iron starvation. Molecular Microbiology. 2011;80:
1071 286–289. doi:10.1111/j.1365-2958.2011.07594.x

1072 95. Martin JE, Imlay JA. The alternative aerobic ribonucleotide reductase of Escherichia coli,
1073 NrdEF, is a manganese-dependent enzyme that enables cell replication during periods of
1074 iron starvation. Molecular Microbiology. 2011;80: 319–334. doi:10.1111/j.1365-
1075 2958.2011.07593.x

1076 96. Outten FW, Wood MJ, Muñoz FM, Storz G. The SufE Protein and the SufBCD Complex
1077 Enhance SufS Cysteine Desulfurase Activity as Part of a Sulfur Transfer Pathway for Fe-S
1078 Cluster Assembly in *Escherichia coli*. J Biol Chem. 2003;278: 45713–45719.
1079 doi:10.1074/jbc.M308004200

1080 97. Monje-Casas F, Jurado J, Prieto-Álamo M-J, Holmgren A, Pueyo C. Expression Analysis
1081 of the *nrdHIEF* Operon from *Escherichia coli*: CONDITIONS THAT TRIGGER THE
1082 TRANSCRIPT LEVEL *IN VIVO*. J Biol Chem. 2001;276: 18031–18037.
1083 doi:10.1074/jbc.M011728200

1084 98. Panosa A, Roca I, Gibert I. Ribonucleotide Reductases of Salmonella Typhimurium:
1085 Transcriptional Regulation and Differential Role in Pathogenesis. Dobrindt U, editor.
1086 PLoS ONE. 2010;5: e11328. doi:10.1371/journal.pone.0011328

1087 99. Troxell B, Hassan HM. Transcriptional regulation by Ferric Uptake Regulator (Fur) in
1088 pathogenic bacteria. Front Cell Infect Microbiol. 2013;3. doi:10.3389/fcimb.2013.00059

1089 100. Colgan AM, Kröger C, Diard M, Hardt W-D, Puente JL, Sivasankaran SK, et al. The
1090 Impact of 18 Ancestral and Horizontally-Acquired Regulatory Proteins upon the
1091 Transcriptome and sRNA Landscape of Salmonella enterica serovar Typhimurium. PLoS
1092 Genet. 2016;12: e1006258. doi:10.1371/journal.pgen.1006258

1093 101. Banerjee R, Weisenhorn E, Schwartz KJ, Myers KS, Glasner JD, Perna NT, et al.
1094 Tailoring a Global Iron Regulon to a Uropathogen. Gottesman S, editor. mBio. 2020;11:
1095 e00351-20, /mbio/11/2/mBio.00351-20.atom. doi:10.1128/mBio.00351-20

1096 102. Hmiel SP, Snavely MD, Miller CG, Maguire ME. Magnesium transport in Salmonella
1097 typhimurium: characterization of magnesium influx and cloning of a transport gene.
1098 Journal of Bacteriology. 1986;168: 1444–1450. doi:10.1128/JB.168.3.1444-1450.1986

1099 103. Snavely MD, Florer JB, Miller CG, Maguire ME. Magnesium transport in Salmonella
1100 typhimurium: Mg2+ transport by the CorA, MgtA, and MgtB systems. Journal of
1101 Bacteriology. 1989;171: 4761–4766. doi:10.1128/JB.171.9.4761-4766.1989

1102 104. Wrande M, Andrews-Polymenis H, Twedt DJ, Steele-Mortimer O, Porwollik S,
1103 McClelland M, et al. Genetic Determinants of Salmonella enterica Serovar Typhimurium
1104 Proliferation in the Cytosol of Epithelial Cells. Infect Immun. 2016;84: 3517–3526.
1105 doi:10.1128/IAI.00734-16

1106 105. Perez-Sepulveda BM, Hinton JCD. Functional Transcriptomics for Bacterial Gene
1107 Detectives. Microbiology Spectrum. 2018;6. doi:10.1128/microbiolspec.RWR-0033-2018

1108 106. Li X, Bleumink-Pluym NMC, Luijkx YMCA, Wubbolts RW, van Putten JPM, Strijbis K.
1109 MUC1 is a receptor for the Salmonella SiiE adhesin that enables apical invasion into
1110 enterocytes. Baumler AJ, editor. PLoS Pathog. 2019;15: e1007566.
1111 doi:10.1371/journal.ppat.1007566

1112 107. Kakhlon O, Cabantchik ZI. The labile iron pool: characterization, measurement, and
1113 participation in cellular processes1 1This article is part of a series of reviews on "Iron and
1114 Cellular Redox Status." The full list of papers may be found on the homepage of the
1115 journal. Free Radical Biology and Medicine. 2002;33: 1037–1046. doi:10.1016/S0891-
1116 5849(02)01006-7

1117 108. Kruszewski M. Labile iron pool: the main determinant of cellular response to oxidative
1118 stress. Mutation Research/Fundamental and Molecular Mechanisms of Mutagenesis.
1119 2003;531: 81–92. doi:10.1016/j.mrfmmm.2003.08.004

1120 109. Tenopoulou M, Kurz T, Doulias P-T, Galaris D, Brunk UT. Does the calcein-AM method
1121 assay the total cellular 'labile iron pool' or only a fraction of it? Biochemical Journal.
1122 2007;403: 261–266. doi:10.1042/BJ20061840

1123 110. Petrat F, de Groot H, Rauen U. Determination of the Chelatable Iron Pool of Single Intact
1124 Cells by Laser Scanning Microscopy. Archives of Biochemistry and Biophysics.
1125 2000;376: 74–81. doi:10.1006/abbi.2000.1711

1126 111. Troxell B, Fink RC, Porwollik S, McClelland M, Hassan HM. The Fur regulon in
1127 anaerobically grown Salmonella enterica sv. Typhimurium: identification of new Fur
1128 targets. BMC Microbiol. 2011;11: 236. doi:10.1186/1471-2180-11-236

1129 112. Bjarnason J, Southward CM, Surette MG. Genomic Profiling of Iron-Responsive Genes in
1130 Salmonella enterica Serovar Typhimurium by High-Throughput Screening of a Random
1131 Promoter Library. Journal of Bacteriology. 2003;185: 4973–4982.
1132 doi:10.1128/JB.185.16.4973-4982.2003

1133 113. Ellermeier JR, Slauch JM. Fur Regulates Expression of the Salmonella Pathogenicity
1134 Island 1 Type III Secretion System through HilD. JB. 2008;190: 476–486.
1135 doi:10.1128/JB.00926-07

1136 114. Troxell B, Sikes ML, Fink RC, Vazquez-Torres A, Jones-Carson J, Hassan HM. Fur
1137 Negatively Regulates hns and Is Required for the Expression of HilA and Virulence in
1138 Salmonella enterica Serovar Typhimurium. Journal of Bacteriology. 2011;193: 497–505.
1139 doi:10.1128/JB.00942-10

1140 115. Hautefort I, Proença MJ, Hinton JCD. Single-copy green fluorescent protein gene fusions
1141 allow accurate measurement of Salmonella gene expression in vitro and during infection
1142 of mammalian cells. Appl Environ Microbiol. 2003;69: 7480–7491.
1143 doi:10.1128/aem.69.12.7480-7491.2003

1144 116. Sturm A, Heinemann M, Arnoldini M, Benecke A, Ackermann M, Benz M, et al. The
1145 Cost of Virulence: Retarded Growth of Salmonella Typhimurium Cells Expressing Type
1146 III Secretion System 1. Ausubel FM, editor. PLoS Pathog. 2011;7: e1002143.
1147 doi:10.1371/journal.ppat.1002143

1148 117. Joseph B, Przybilla K, Stühler C, Schauer K, Slaghuis J, Fuchs TM, et al. Identification of
1149 Listeria monocytogenes Genes Contributing to Intracellular Replication by Expression
1150 Profiling and Mutant Screening. Journal of Bacteriology. 2006;188: 556–568.
1151 doi:10.1128/JB.188.2.556-568.2006

1152 118. Chatterjee SS, Hossain H, Otten S, Kuenne C, Kuchmina K, Machata S, et al. Intracellular
1153 Gene Expression Profile of Listeria monocytogenes. Infect Immun. 2006;74: 1323–1338.
1154 doi:10.1128/IAI.74.2.1323-1338.2006

1155 119. Alpuche Aranda CM, Swanson JA, Loomis WP, Miller SI. Salmonella typhimurium
1156 activates virulence gene transcription within acidified macrophage phagosomes. Proc Natl
1157 Acad Sci U S A. 1992;89: 10079–10083. doi:10.1073/pnas.89.21.10079

1158 120. Rathman M, Sjaastad MD, Falkow S. Acidification of phagosomes containing Salmonella
1159 typhimurium in murine macrophages. Infect Immun. 1996;64: 2765–2773.
1160 doi:10.1128/IAI.64.7.2765-2773.1996

1161 121. Garcia-del Portillo F, Foster JW, Maguire ME, Finlay BB. Characterization of the micro-
1162 environment of Salmonella typhimurium-containing vacuoles within MDCK epithelial
1163 cells. Mol Microbiol. 1992;6: 3289–3297.

1164 122. Liu Y, Zhang Q, Hu M, Yu K, Fu J, Zhou F, et al. Proteomic Analyses of Intracellular
1165 Salmonella enterica Serovar Typhimurium Reveal Extensive Bacterial Adaptations to
1166 Infected Host Epithelial Cells. Payne SM, editor. Infect Immun. 2015;83: 2897–2906.
1167 doi:10.1128/IAI.02882-14

1168 123. Avraham R, Haseley N, Brown D, Penaranda C, Jijon HB, Trombetta JJ, et al. Pathogen
1169 Cell-to-Cell Variability Drives Heterogeneity in Host Immune Responses. Cell. 2015;162:
1170 1309–1321. doi:10.1016/j.cell.2015.08.027

1171 124. Saliba A-E, Li L, Westermann AJ, Appenzeller S, Stapels DAC, Schulte LN, et al. Single-
1172 cell RNA-seq ties macrophage polarization to growth rate of intracellular Salmonella. Nat
1173 Microbiol. 2017;2: 16206. doi:10.1038/nmicrobiol.2016.206

1174 125. Hoiseth SK, Stocker BAD. Aromatic-dependent Salmonella typhimurium are non-virulent
1175 and effective as live vaccines. Nature. 1981;291: 238–239. doi:10.1038/291238a0

1176 126. Edwards RA, Keller LH, Schifferli DM. Improved allelic exchange vectors and their use
1177 to analyze 987P fimbria gene expression. Gene. 1998;207: 149–157. doi:10.1016/S0378-
1178 1119(97)00619-7

1179 127. Datsenko KA, Wanner BL. One-step inactivation of chromosomal genes in Escherichia
1180 coli K-12 using PCR products. Proc Natl Acad Sci USA. 2000;97: 6640–6645.
1181 doi:10.1073/pnas.120163297

1182 128. Porwollik S, Santiviago CA, Cheng P, Long F, Desai P, Fredlund J, et al. Defined Single-
1183 Gene and Multi-Gene Deletion Mutant Collections in Salmonella enterica sv
1184 Typhimurium. Hensel M, editor. PLoS ONE. 2014;9: e99820.
1185 doi:10.1371/journal.pone.0099820

1186 129. Lawley TD, Chan K, Thompson LJ, Kim CC, Govoni GR, Monack DM. Genome-Wide
1187 Screen for Salmonella Genes Required for Long-Term Systemic Infection of the Mouse.
1188 PLoS Pathog. 2006;2: e11. doi:10.1371/journal.ppat.0020011

1189 130. Knodler LA, Crowley SM, Sham HP, Yang H, Wrande M, Ma C, et al. Noncanonical
1190 inflammasome activation of caspase-4/caspase-11 mediates epithelial defenses against
1191 enteric bacterial pathogens. Cell Host Microbe. 2014;16: 249–256.
1192 doi:10.1016/j.chom.2014.07.002

1193 131. Rollenhagen C, Sorensen M, Rizos K, Hurvitz R, Bumann D. Antigen selection based on
1194 expression levels during infection facilitates vaccine development for an intracellular
1195 pathogen. Proceedings of the National Academy of Sciences. 2004;101: 8739–8744.
1196 doi:10.1073/pnas.0401283101

1197 132. Ibarra JA, Knodler LA, Sturdevant DE, Virtaneva K, Carmody AB, Fischer ER, et al.
1198 Induction of Salmonella pathogenicity island 1 under different growth conditions can
1199 affect Salmonella-host cell interactions in vitro. Microbiology (Reading, Engl). 2010;156:
1200 1120–1133. doi:10.1099/mic.0.032896-0

1201 133. Holly MK, Han X, Zhao EJ, Crowley SM, Allaire JM, Knodler LA, et al. *Salmonella*
1202 *enterica* infection of murine and human enteroid-derived monolayers elicits differential
1203 activation of epithelial-intrinsic inflammasomes. Infect Immun. 2020; IAI.00017-20,
1204 iai;IAI.00017-20v1. doi:10.1128/IAI.00017-20

1205 134. Klein JA, Powers TR, Knodler LA. Measurement of Salmonella enterica Internalization
1206 and Vacuole Lysis in Epithelial Cells. Methods Mol Biol. 2017;1519: 285–296.
1207 doi:10.1007/978-1-4939-6581-6_19

1208 135. Hoffmann S, Otto C, Kurtz S, Sharma CM, Khaitovich P, Vogel J, et al. Fast mapping of
1209 short sequences with mismatches, insertions and deletions using index structures. PLoS
1210 Comput Biol. 2009;5: e1000502. doi:10.1371/journal.pcbi.1000502

1211 136. Langmead B, Salzberg SL. Fast gapped-read alignment with Bowtie 2. Nat Methods.
1212 2012;9: 357–359. doi:10.1038/nmeth.1923

1213 137. Li B, Dewey CN. RSEM: accurate transcript quantification from RNA-Seq data with or
1214 without a reference genome. BMC Bioinformatics. 2011;12: 323. doi:10.1186/1471-2105-
1215 12-323

1216 138. Glaus P, Honkela A, Rattray M. Identifying differentially expressed transcripts from
1217 RNA-seq data with biological variation. Bioinformatics. 2012;28: 1721–1728.
1218 doi:10.1093/bioinformatics/bts260

1219 139. Breitling R, Armengaud P, Amtmann A, Herzyk P. Rank products: a simple, yet powerful,
1220 new method to detect differentially regulated genes in replicated microarray experiments.
1221 FEBS Letters. 2004;573: 83–92. doi:10.1016/j.febslet.2004.07.055

1222 140. Hong F, Breitling R, McEntee CW, Wittner BS, Nemhauser JL, Chory J. RankProd: a
1223 bioconductor package for detecting differentially expressed genes in meta-analysis.
1224 Bioinformatics. 2006;22: 2825–2827. doi:10.1093/bioinformatics/btl476

1225 141. Smith C, Stringer AM, Mao C, Palumbo MJ, Wade JT. Mapping the Regulatory Network
1226 for Salmonella enterica Serovar Typhimurium Invasion. MBio. 2016;7.
1227 doi:10.1128/mBio.01024-16

1228 142. Fink RC, Evans MR, Porwollik S, Vazquez-Torres A, Jones-Carson J, Troxell B, et al.
1229 FNR Is a Global Regulator of Virulence and Anaerobic Metabolism in Salmonella enterica
1230 Serovar Typhimurium (ATCC 14028s). Journal of Bacteriology. 2007;189: 2262–2273.
1231 doi:10.1128/JB.00726-06

1232

1233

1234 **Figure Legends**

1235 **Fig 1. EBSS and wortmannin inversely affect the cytosolic population.** (A) Schematic of the
1236 experimental design employed to differentially modulate host cell autophagy. (B) Epithelial cells
1237 seeded on glass coverslips were pretreated with EBSS or 100 nM WTM as depicted in (A) and
1238 infected with *S*. Typhimurium wild-type bacteria harboring pFPV-mCherry for plasmid-borne,
1239 constitutive expression of *mCherry*. The proportion of bacteria accessible to anti-*Salmonella* LPS
1240 antibodies delivered to the mammalian cell cytosol was determined by digitonin permeabilization
1241 assay and fluorescence microscopy. n≥3 independent experiments (C) Epithelial cells seeded on
1242 coverslips were pretreated as in (A) and infected with mCherry-S. Typhimurium (wild-type
1243 *glmS*::P*trc-mCherrySST*::FRT bacteria constitutively expressing a chromosomal copy of *mCherry*)
1244 harboring the fluorescent reporter plasmid, P*uhpT-gfpova* (pNF101). At the indicated times, cells
1245 were fixed and the proportion of infected cells containing cytosolic bacteria (GFP-positive) was
1246 scored by fluorescence microscopy. n=3 independent experiments. (D) Cells seeded on
1247 coverslips were pretreated as in (A) and infected with wild-type bacteria harboring pFPV-mCherry.
1248 The number of bacteria in each infected cell was scored by fluorescence microscopy. Cells with
1249 ≥100 bacteria contain cytosolic *S*. Typhimurium. Each dot represents one infected cell. n=2 (1 h)
1250 or 3 (8 h) independent experiments. (E) Epithelial cells were infected with wild-type bacteria and
1251 the number of intracellular bacteria at 1 h and 8 h p.i. was determined by gentamicin protection
1252 assay. Fold-replication is CFUs at 8 h/1 h. n=3 independent experiments. For all panels, control
1253 = untreated cells; EBSS = Earle's balanced salt solution treatment; WTM = wortmannin treatment.
1254

1255 **Fig 2. Pathway enrichment analysis results for the RNA-seq analysis.** Top panels indicate
1256 regulons generated from transcriptional profiling of key regulatory mutants, while bottom panels
1257 display enriched gene sets generated from KEGG, GO, or from RNA-seq profiling of *S.*
1258 Typhimurium under 22 infection-relevant *in vitro* growth conditions. All displayed enrichments are
1259 significant (adjusted p-value <0.05) according to Fisher's exact test with Benjamini-Hochberg

1260 correction for multiple comparisons. The number of genes/sRNAs in each category is shown in
1261 log_2 scale. Only a selection of non-redundant pathways is presented; the full data set is available
1262 in S2 Table.
1263
1264 **Fig 3. Iron-associated genes/sRNAs are induced in the epithelial cytosol.** (A) Epithelial cells
1265 seeded on coverslips were infected wild-type mCherry-*S*. Typhimurium harboring fluorescent
1266 transcriptional reporters. The promoter region of each gene of interest was inserted upstream of
1267 a promoterless *gfpmut3*. At 8 h p.i., cells were fixed and stained with Hoechst 33342 to detect
1268 DNA. Representative confocal microscopy images show induction of *iroB*, *nrdH*, *sitA*, *sufA*, *yjjZ*
1269 and *STnc3080* promoters in cytosolic bacteria. Green = transcriptional reporter, red = *S*.
1270 Typhimurium, blue = DNA. Scale bars are 10 μm. (B) Quantification of the mean fluorescence
1271 intensity (MFI) of GFP signal in individual bacteria. Bacteria were designated as being cytosolic
1272 (Cyto) or vacuolar (Vac) if residing within cells with ≥100 bacteria or 2-40 bacteria, respectively.
1273 Each dot represents one bacterium. Solid black line indicates the mean. Acquisition parameters
1274 (acquisition time and gain) were set up using P*sitA-gfpmut3* (the highest GFP intensity) and these
1275 same parameters were applied throughout. The MFI for each bacterium was determine using
1276 ImageJ. Dashed lines indicate the range of background fluorescence in the GFP channel
1277 measured for mCherry-*S*. Typhimurium (no reporter). n=2 independent experiments.
1278
1279 **Fig 4. Manipulation of cellular iron levels primarily affects cytosolic bacteria.** (A) Epithelial
1280 cells seeded on coverslips were left untreated (control) or treated overnight in growth media
1281 supplemented with 10 μM, 30 μM, 100 μM or 300 μM ferric ammonium citrate (FAC). Cells were
1282 infected with wild-type mCherry-*S*. Typhimurium harboring P*iroN-gfpmut3*, P*sitA-gfpmut3* or
1283 P*yjjZ-gfpmut3* reporters, fixed at 8 h p.i. and the MFI of GFP signal in individual bacteria was
1284 quantified by fluorescence microscopy. Bacteria were designated as being cytosolic (Cyto) or
1285 vacuolar (Vac) if residing within cells with ≥100 bacteria or 2-40 bacteria, respectively. Each dot

1286 represents one bacterium. Solid black line indicates the mean. Acquisition parameters (acquisition
1287 time and gain) were set-up using P*iroN-gfpmut3* (the highest GFP intensity) and these same
1288 parameters were applied throughout. The MFI for each bacterium was determine using ImageJ.
1289 Dashed lines indicate the range of background fluorescence in the GFP channel measured for
1290 mCherry-*S*. Typhimurium (no reporter). n=2 independent experiments. (B) Epithelial cells seeded
1291 on coverslips were left untreated (control) or treated overnight with growth media containing 200
1292 μM 2,2-dipyridyl (DPI), a metal-chelating compound, 200 μM DPI + 200 μM ferric ammonium
1293 citrate (DPI+FAC) or 200 μM FAC alone (FAC). Infection strains and quantification of GFP signal
1294 were as described for (A). n=2 independent experiments. (C) Cells were treated as in (B) and
1295 infected with wild-type bacteria. The number of intracellular bacteria was quantified by gentamicin
1296 protection assay at 1 h and 8 h p.i. Fold-replication is CFUs at 8 h/1 h. n=3 experiments. (D) Cells
1297 were treated as in (B) and infected with wild-type bacteria. The proportion of cytosolic bacteria
1298 was quantified by CHQ resistance assay at Fig 6 h p.i. n≥3 experiments. (E) Cells were treated
1299 as in (B) and infected with mCherry-*S*. Typhimurium harboring a plasmid-borne reporter of
1300 cytosolic access, pNF101, and fixed at 8 h p.i. Left panel: the proportion of infected cells
1301 containing only cytosolic (all bacteria are GFP-positive, mCherry-positive), only vacuolar (all
1302 bacteria are GFP-negative, mCherry-positive) or a mixed population (Cyto+Vac) of bacteria was
1303 blindly scored by fluorescence microscopy. n≥5 independent experiments. Right panel: the
1304 number of cytosolic or vacuolar bacteria in each cell was scored. Horizontal black lines indicate
1305 the mean number of bacteria/cell. Cumulative data from two independent experiments is shown.
1306

1307 **Fig 5. Zn^{2+} and Mg^{2+} are limiting in the vacuole, not the cytosol.** Upper panels: Epithelial cells
1308 seeded on coverslips were infected with mCherry-*S*. Typhimurium harboring P*zinT-gfpmut3* or
1309 P*mgtC-gfpmut3* transcriptional reporters. At 8 h p.i., cells were fixed and stained with Hoechst
1310 33342 to detect DNA. Representative confocal microscopy images show induction of *zinT* (upper
1311 panel) *and mgtC* (lower panel) promoters in vacuolar bacteria. Green = transcriptional reporter,

1312 red = *S*. Typhimurium, blue = DNA. Scale bars are 10 μm. Lower panels: Quantification of the
1313 MFI of GFP signal in individual bacteria. Bacteria were designated as being cytosolic (Cyto) or
1314 vacuolar (Vac) if residing within cells with ≥100 bacteria or 2-40 bacteria, respectively. Each dot
1315 represents one bacterium. Solid black line indicates the mean. Acquisition parameters (acquisition
1316 time and gain) were set-up using P*zinT-gfpmut3* (the highest GFP intensity) and these same
1317 parameters were applied throughout. The MFI for each bacterium was determine using ImageJ.
1318 Dashed lines indicate the range of background fluorescence in the GFP channel measured for
1319 mCherry-*S*. Typhimurium (no reporter). n=2 independent experiments.
1320
1321 **Fig 6. SPI1-associated genes are specifically up-regulated in the epithelial cytosol.** (A)
1322 Epithelial cells seeded on coverslips were infected with mCherry-*S*. Typhimurium harboring
1323 *gfpmut3* transcriptional reporters. At 8 h p.i., cells were fixed and stained with Hoechst 33342 to
1324 detect DNA. Representative confocal microscopy images show induction of *sicA*, *sopE2*, *sopF*,
1325 *siiA* and *lpxR* promoters in cytosolic bacteria. PipB is a type III effector translocated by T3SS2
1326 and the P*pipB-gfpmut3* reporter served as a control for vacuole-specific gene induction. Green =
1327 transcriptional reporter, red = *S*. Typhimurium, blue = DNA. Scale bars are 10 μm. (B)
1328 Quantification of the mean fluorescence intensity (MFI) of GFP signal in individual bacteria.
1329 Bacteria were designated as being cytosolic (Cyto) or vacuolar (Vac) if residing within cells with
1330 ≥100 bacteria or 2-40 bacteria, respectively. Each dot represents one bacterium; solid black line
1331 indicates the mean. Acquisition parameters (acquisition time and gain) were set-up using P*sicA-*
1332 *gfpmut3* (the highest GFP intensity) and these same parameters were applied throughout. The
1333 MFI for each bacterium was determine using ImageJ. Dashed lines indicate the range of
1334 background fluorescence in the GFP channel measured for mCherry-*S*. Typhimurium (no
1335 reporter). n=2 independent experiments.
1336

1337 **Fig 7. A subset of up-regulated genes is required for optimal proliferation in the cytosol.**
1338 (A) Epithelial cells were infected with wild-type (WT) bacteria or the indicated gene deletion
1339 mutants and the proportion of cytosolic bacteria at Fig 6 h p.i. was quantified using the CHQ
1340 resistance assay. n≥5 independent experiments. (B) Epithelial cells seeded on coverslips were
1341 infected with WT bacteria or gene deletion mutant harboring pCHAR-Duo(ASV), a plasmid-borne
1342 dual reporter – constitutive *mCherry* expression is driven by the synthetic ProB promoter and
1343 *gfpmut3.1(ASV)* (encoding for destabilized GFP) is under the control of the glucose-6-phosphate
1344 responsive *uhpT* promoter from *S*. Typhimurium. The proportion of infected cells at 8 h p.i.
1345 containing only cytosolic (all bacteria are GFP-positive, mCherry-positive), only vacuolar (all
1346 bacteria are GFP-negative, mCherry-positive) or a mixed population (cytosolic and vacuolar) of
1347 bacteria was blindly scored by fluorescence microscopy. n=4 experiments.
1348

1349 **Supporting Information**

1350 **Dataset S1 (separate file).** RNA-seq data set. All genes/sRNAs with mapped reads were
1351 reported as TPM and a threshold TPM value of 10 was used as a cut-off to distinguish gene
1352 expression from background. Genes/sRNAs were deemed differentially expressed using fold-
1353 change criteria of ≥1.40 (cytosol up-regulated) and ≤0.71 (vacuole up-regulated) for WTM/EBSS
1354 treatment conditions (cells highlighted in yellow in Tab 1). Statistical significance was assessed
1355 using two independent platforms, Bayesian interference of transcripts from sequencing data
1356 (BitSeq) and rank products (RankProduct). For Bitseq analysis, we arbitrarily set a Probability of
1357 Positive Log Ratio (PPLR) of ≥0.90 for "up cytosol" genes/sRNAs and ≤0.1 for "up vacuole"
1358 genes/sRNAs for statistical significance (cells highlighted in green in Tab 1). For RankProduct
1359 analysis, the cutoff for differentially expressed genes was arbitrarily set to a percentage of false
1360 positive (pfp) value of ≤0.2 (cells highlighted in green in Tab 1) for statistical significance. Tab 2
1361 is the short list of "up cytosol" genes/sRNAs that passed statistical significance. Tab 3 is the
1362 short-list of "up vacuole" genes/sRNAs that passed statistical significance. Expression profiles of
1363 these genes/sRNAs in 22 distinct infection-relevant *in vitro* growth conditions is shown in Tab 2
1364 and Tab 3 (http://bioinf.gen.tcd.ie/cgi-bin/salcom.pl?db=salcom_mac_HL).

1365

1366 **Dataset 2 (separate file).** Custom pathway enrichment analysis of "up cytosol" and "up
1367 vacuole" genes/sRNAs. Tab 1 represents the curated list shown in Figure 2. Tab 2 shows the
1368 starting entire dataset.

1369

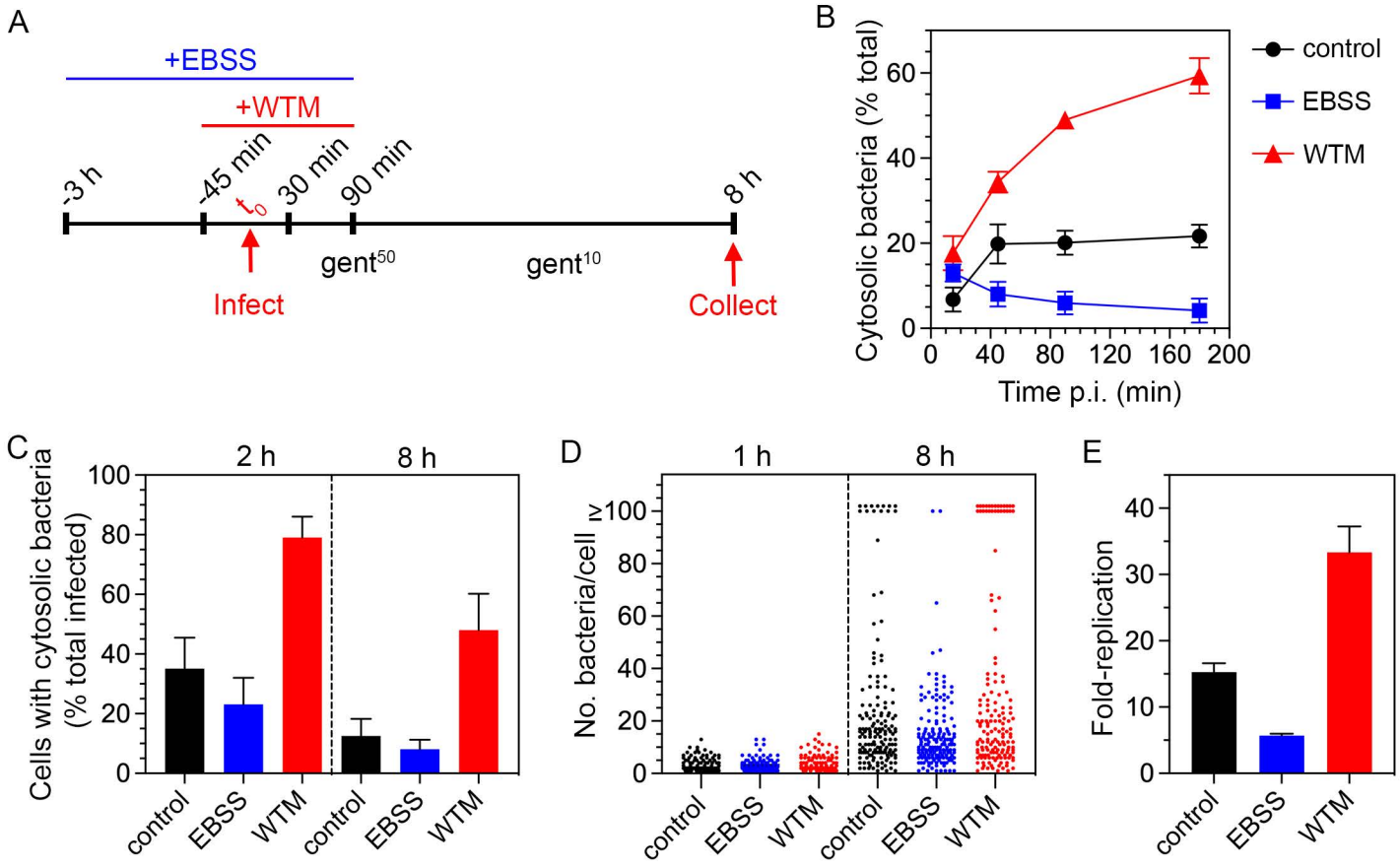
A
+EBSS
+WTM
-3 h
-45 min
t_0
30 min
90 min
8 h
gent50
gent10
Infect
Collect
B
Cytosolic bacteria (% total)
Time p.i. (min)
control
EBSS
WTM
C
Cells with cytosolic bacteria (% total infected)
2 h
8 h
control
EBSS
WTM
D
No. bacteria/cell
1 h
8 h
E
Fold-replication

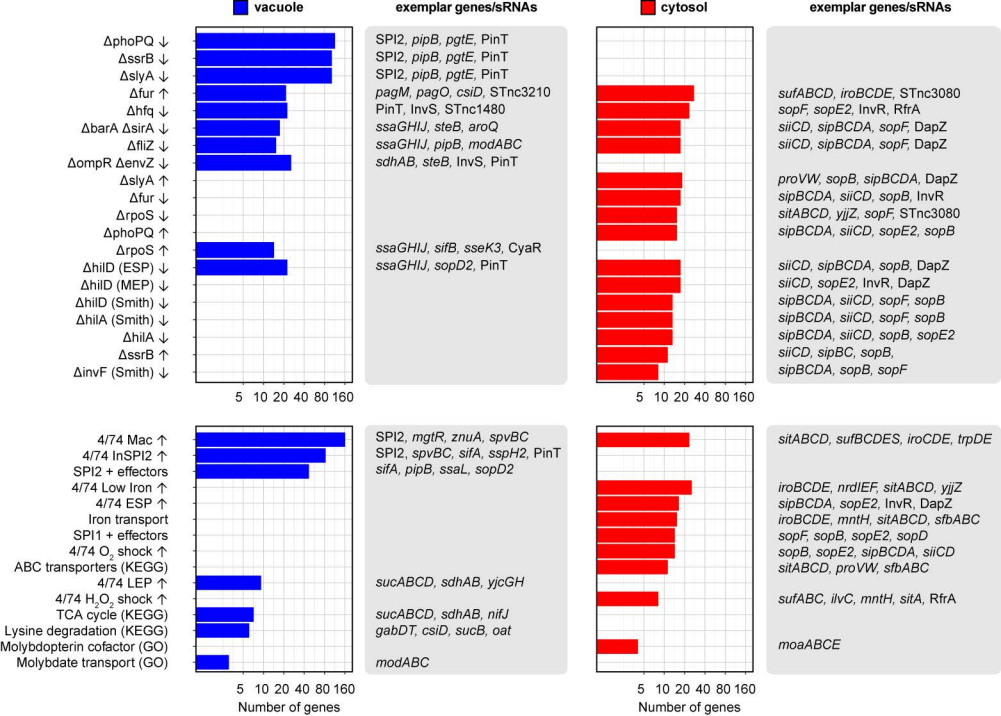
vacuole
exemplar genes/sRNAs
cytosol
exemplar genes/sRNAs
ΔphoPQ ↓
ΔssrB ↓
ΔslyA ↓
Δfur ↑
Δhfq ↓
ΔbarA ΔsirA ↓
ΔfliZ ↓
ΔompR ΔenvZ ↓
ΔslyA ↑
Δfur ↓
ΔrpoS ↓
ΔphoPQ ↑
ΔrpoS ↑
ΔhilD (ESP) ↓
ΔhilD (MEP) ↓
ΔhilD (Smith) ↓
ΔhilA (Smith) ↓
ΔhilA ↓
ΔssrB ↑
ΔinvF (Smith) ↓
SPI2, pipB, pgtE, PinT
SPI2, pipB, pgtE, PinT
SPI2, pipB, pgtE, PinT
pagM, pagO, csiD, STnc3210
PinT, InvS, STnc1480
ssaGHIJ, steB, aroQ
ssaGHIJ, pipB, modABC
sdhAB, steB, InvS, PinT
ssaGHIJ, sifB, sseK3, CyaR
ssaGHIJ, sopD2, PinT
sufABCD, iroBCDE, STnc3080
sopF, sopE2, InvR, RfrA
siiCD, sipBCDA, sopF, DapZ
siiCD, sipBCDA, sopF, DapZ
proVW, sopB, sipBCDA, DapZ
sipBCDA, siiCD, sopB, InvR
sitABCD, yjjZ, sopF, STnc3080
sipBCDA, siiCD, sopE2, sopB
siiCD, sipBCDA, sopB, DapZ
siiCD, sopE2, InvR, DapZ
sipBCDA, siiCD, sopF, sopB
sipBCDA, siiCD, sopF, sopB
sipBCDA, siiCD, sopB, sopE2
siiCD, sipBC, sopB,
sipBCDA, sopB, sopF
5 10 20 40 80 160
4/74 Mac ↑
4/74 InSPI2 ↑
SPI2 + effectors
4/74 Low Iron ↑
4/74 ESP ↑
Iron transport
SPI1 + effectors
4/74 O2 shock ↑
ABC transporters (KEGG)
4/74 LEP ↑
4/74 H2O2 shock ↑
TCA cycle (KEGG)
Lysine degradation (KEGG)
Molybdopterin cofactor (GO)
Molybdate transport (GO)
SPI2, mgtR, znuA, spvBC
SPI2, spvBC, sifA, sspH2, PinT
sifA, pipB, ssaL, sopD2
sucABCD, sdhAB, yjcGH
sucABCD, sdhAB, nifJ
gabDT, csiD, sucB, oat
modABC
sitABCD, sufBCDES, iroCDE, trpDE
iroBCDE, nrdIEF, sitABCD, yjjZ
sipBCDA, sopE2, InvR, DapZ
iroBCDE, mntH, sitABCD, sfbABC
sopF, sopB, sopE2, sopD
sopB, sopE2, sipBCDA, siiCD
sitABCD, proVW, sfbABC
sufABC, ilvC, mntH, sitA, RfrA
moaABCE
Number of genes
Number of genes

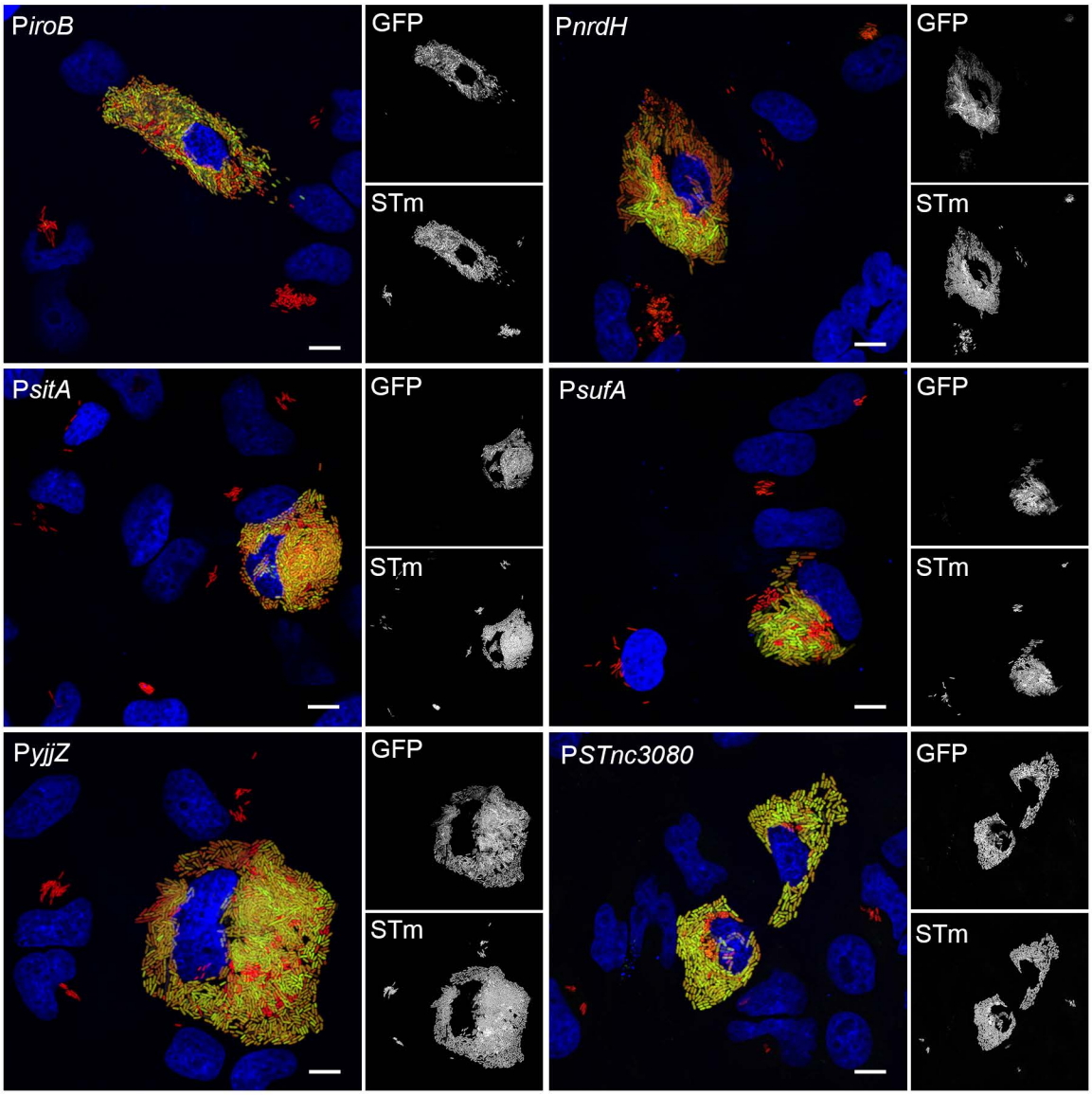
PiroB
GFP
STm
PnrdH
GFP
STm
PsitA
GFP
STm
PsufA
GFP
STm
PyjjZ
GFP
STm
PSTnc3080
GFP
STm

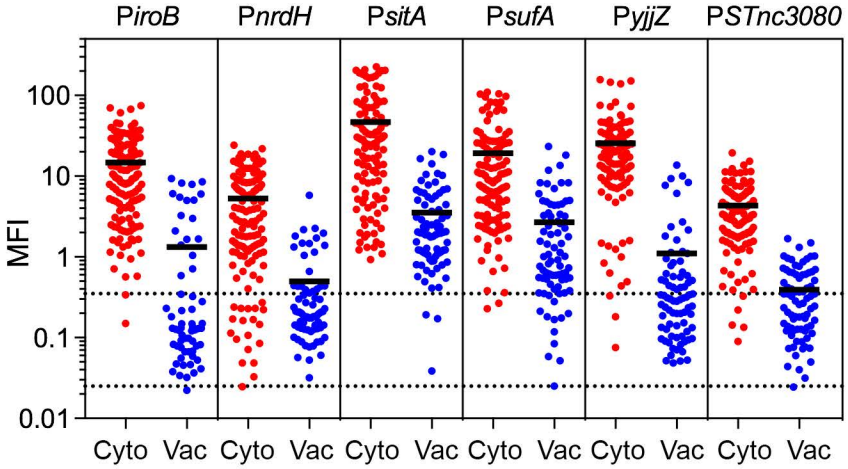
PiroB
PnrdH
PsitA
PsufA
PyjjZ
PSTnc3080
MFI
100
10
1
0.1
0.01
Cyto
Vac
Cyto
Vac
Cyto
Vac
Cyto
Vac
Cyto
Vac
Cyto
Vac

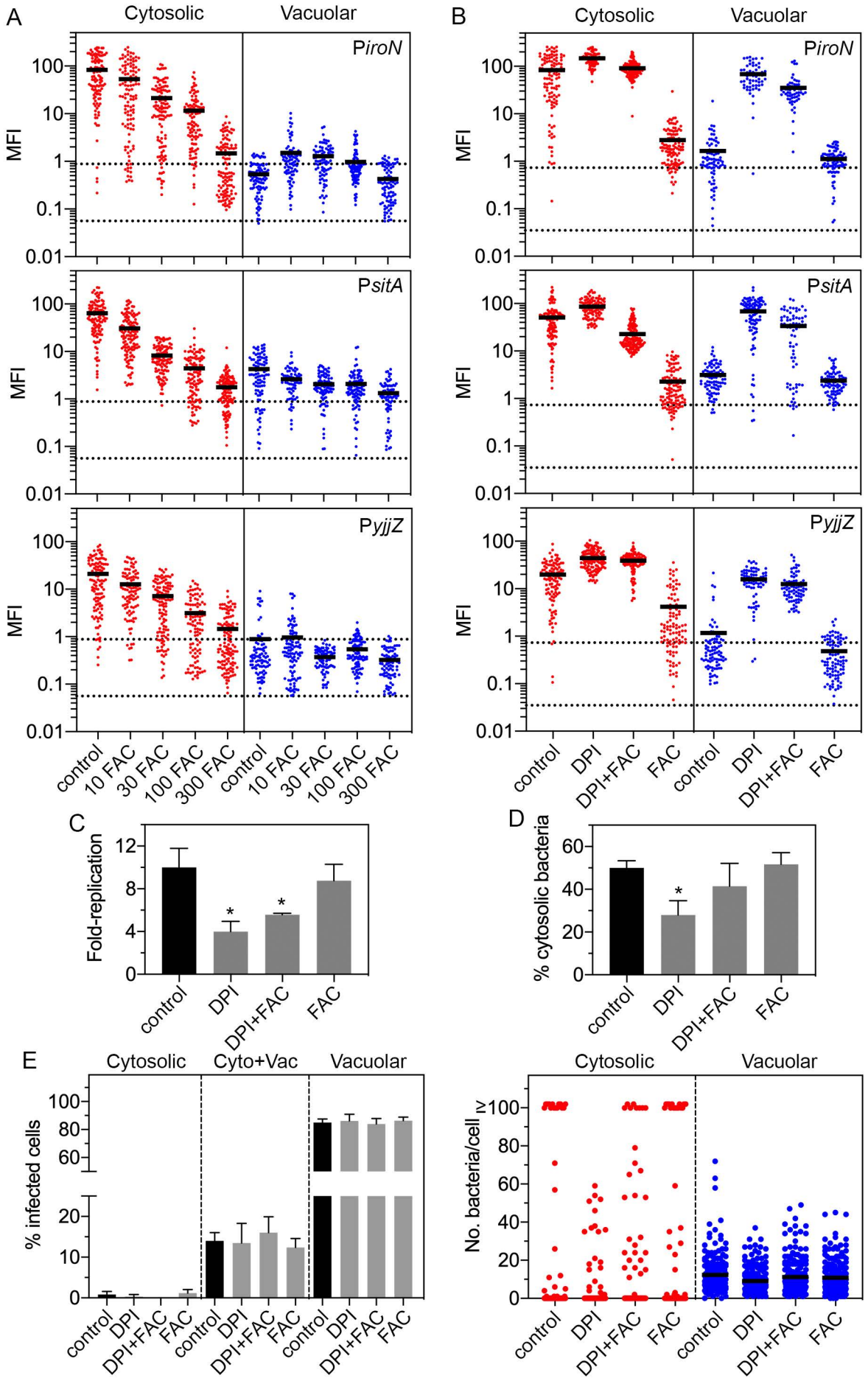
A
Cytosolic
Vacuolar
PiroN
PsitA
PyjjZ
MFI
100
10
1
0.1
0.01
control
10 FAC
30 FAC
100 FAC
300 FAC
B
DPI
DPI+FAC
FAC
C
Fold-replication
12
8
4
0
D
% cytosolic bacteria
60
40
20
E
Cyto+Vac
% infected cells
80
No. bacteria/cell
≥100

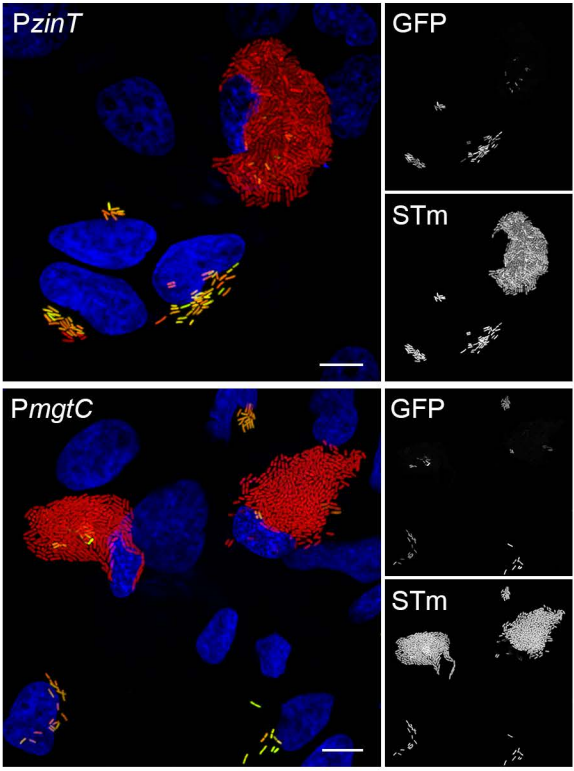
PzinT
GFP
STm
PmgtC
GFP
STm

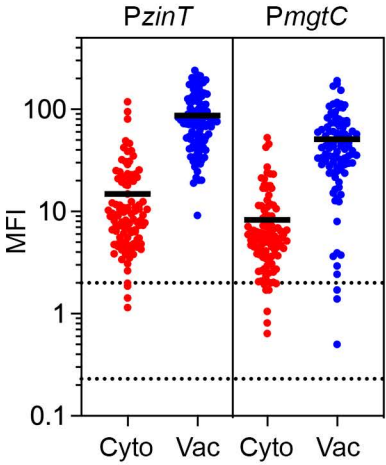
PzinT
PmgtC
MFI
100
10
1
0.1
Cyto
Vac
Cyto
Vac

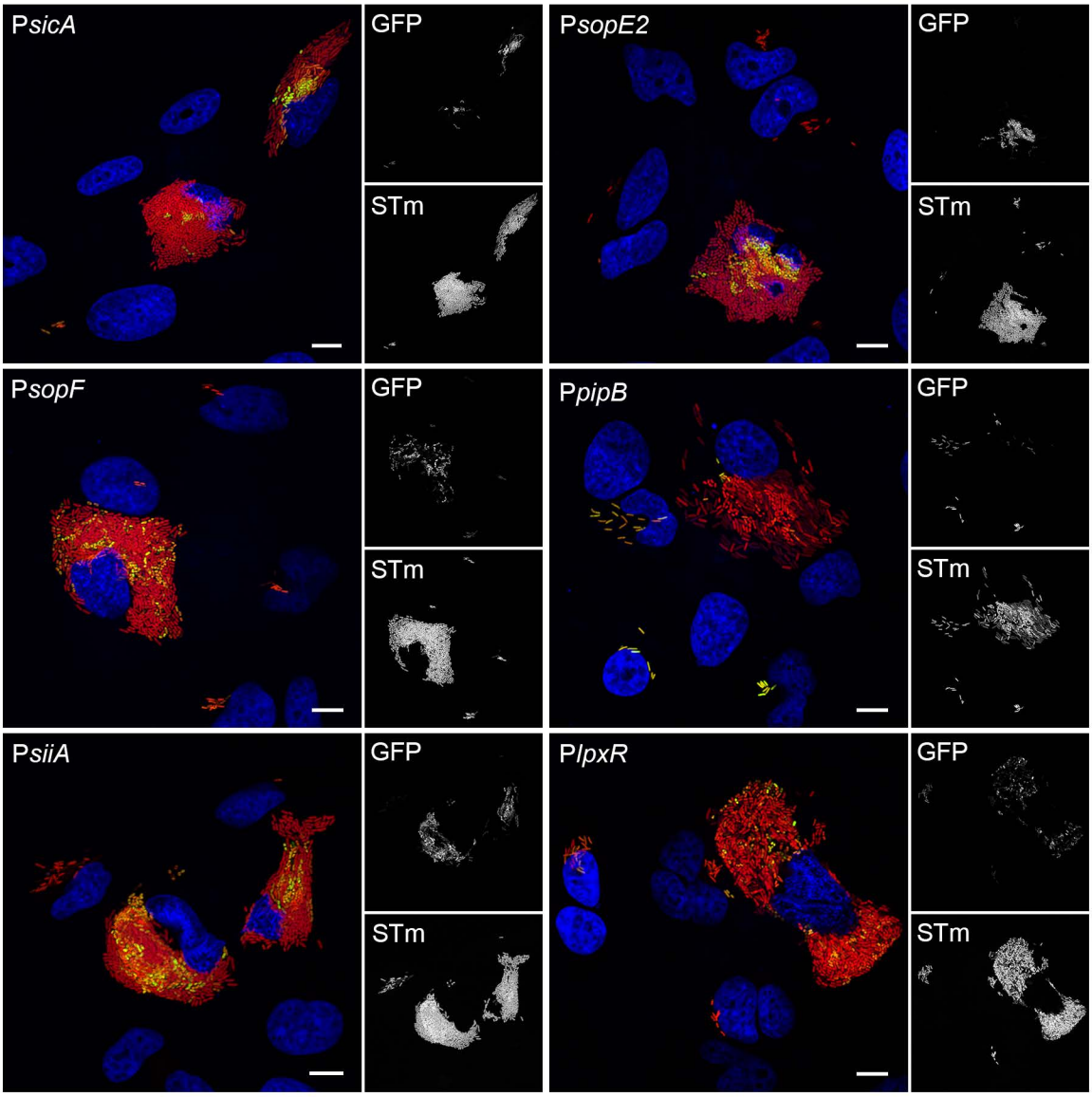
PsicA
GFP
STm
PsopE2
GFP
STm
PsopF
GFP
STm
PpipB
GFP
STm
PsiiA
GFP
STm
PlpxR
GFP
STm

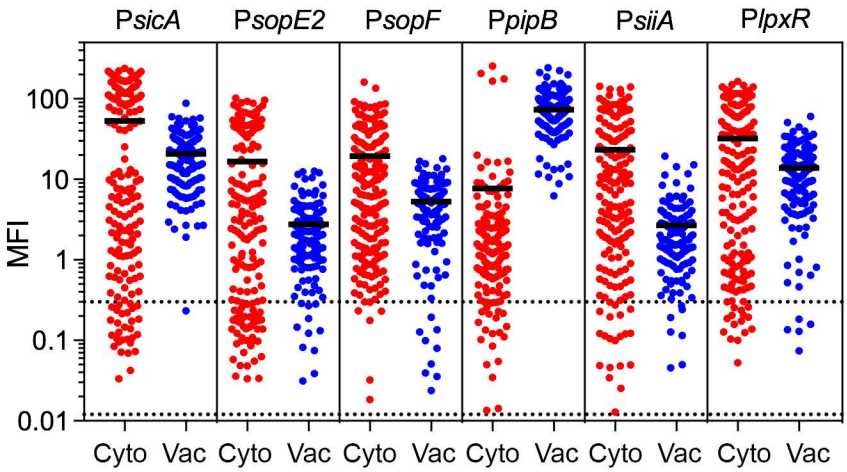
PsicA
PsopE2
PsopF
PpipB
PsiiA
PlpxR
MFI
100
10
1
0.1
0.01
Cyto
Vac
Cyto
Vac
Cyto
Vac
Cyto
Vac
Cyto
Vac
Cyto
Vac

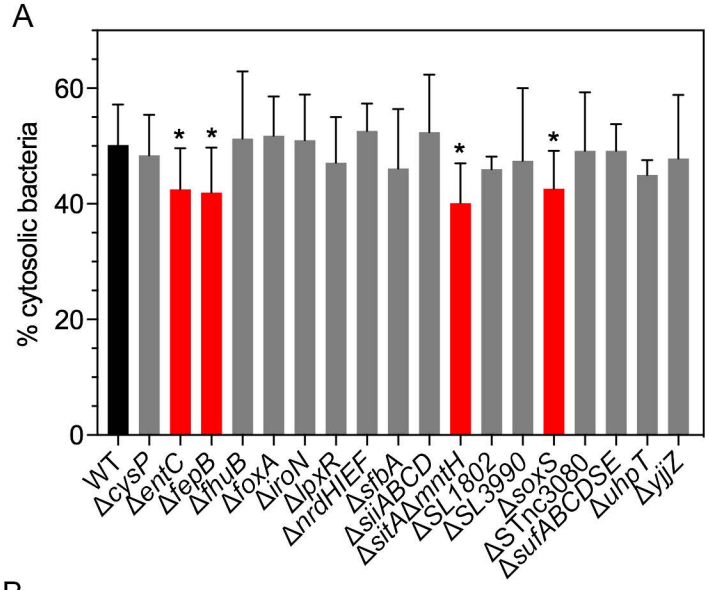
A
% cytosolic bacteria
0
20
40
60
*
*
*
*
WT
ΔcysP
ΔentC
ΔfepB
ΔfhuB
ΔfoxA
ΔiroN
ΔlpxR
ΔnrdHIEF
ΔsrfbA
ΔsiiABCD
ΔsitAΔmntH
ΔSL1802
ΔSL3990
ΔsoxS
ΔSTnc3080
ΔsufABCDSE
ΔuhpT
ΔyjjZ

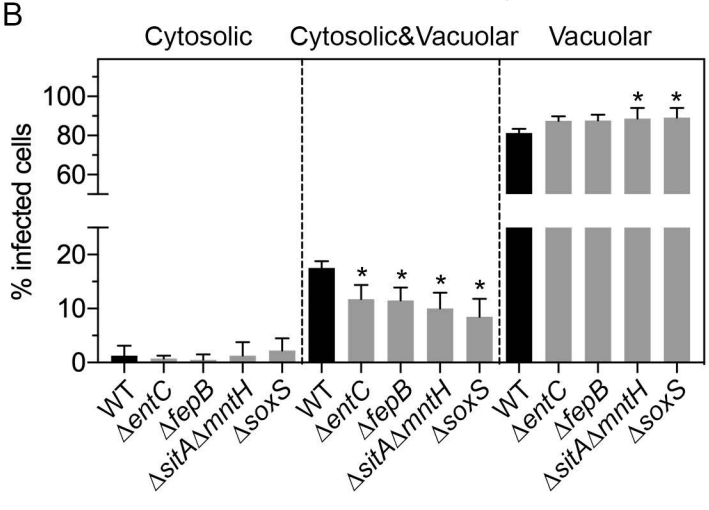
B
Cytosolic
Cytosolic&Vacuolar
Vacuolar
% infected cells
0
10
20
60
80
100
*
*
*
*
*
*
WT
ΔentC
ΔfepB
ΔsitAΔmntH
ΔsoxS
WT
ΔentC
ΔfepB
ΔsitAΔmntH
ΔsoxS
WT
ΔentC
ΔfepB
ΔsitAΔmntH
ΔsoxS

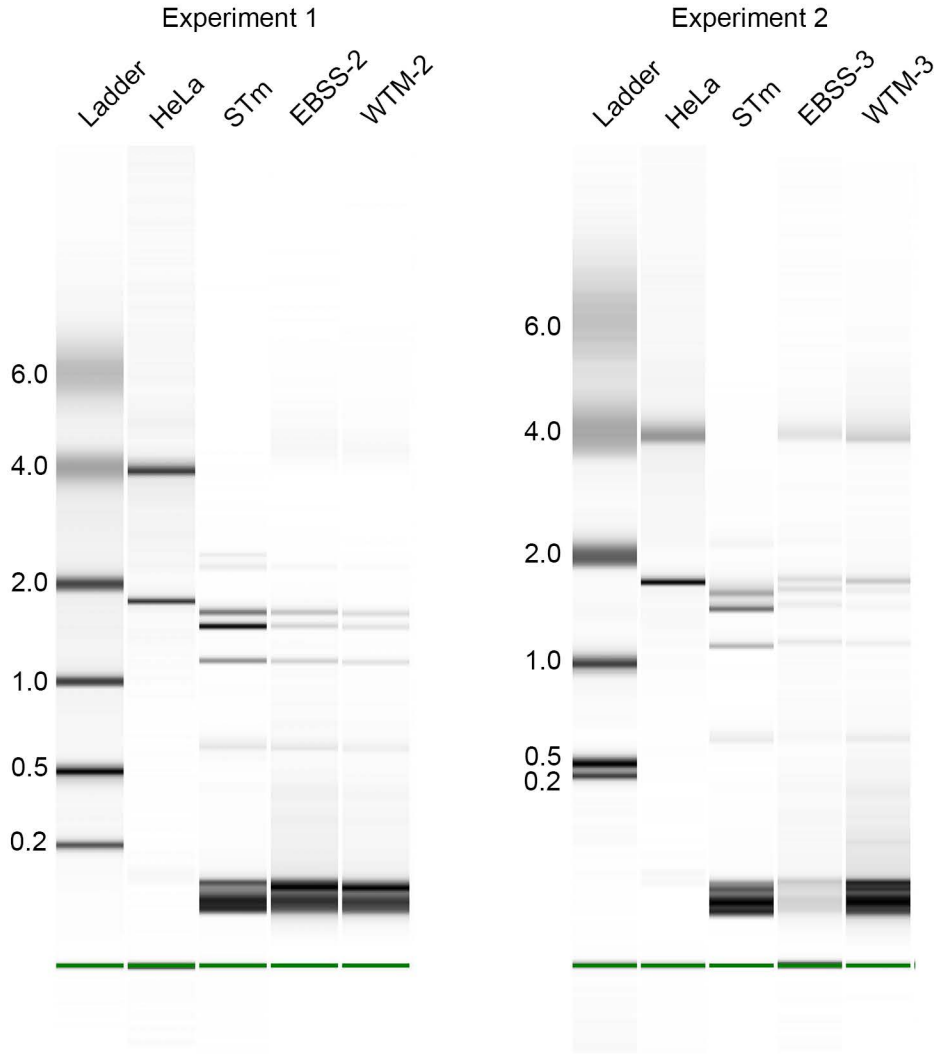

Figure S1. Enrichment of bacterial RNA from infected cells. Total RNA was extracted from HeLa epithelial cells (HeLa), wild-type *S*. Typhimurium SL1344 grown to late log-phase (STm), *S*. Typhimurium isolated from Earle's balance salt solution (EBSS)-treated cells at 8 h p.i. or *S*. Typhimurium isolated from wortmannin (WTM)-treated cells at 8 h p.i. RNA quality was analyzed by electrophoretic separation using an Agilent Bioanalyzer 2100. Ladder sizes shown in kb.

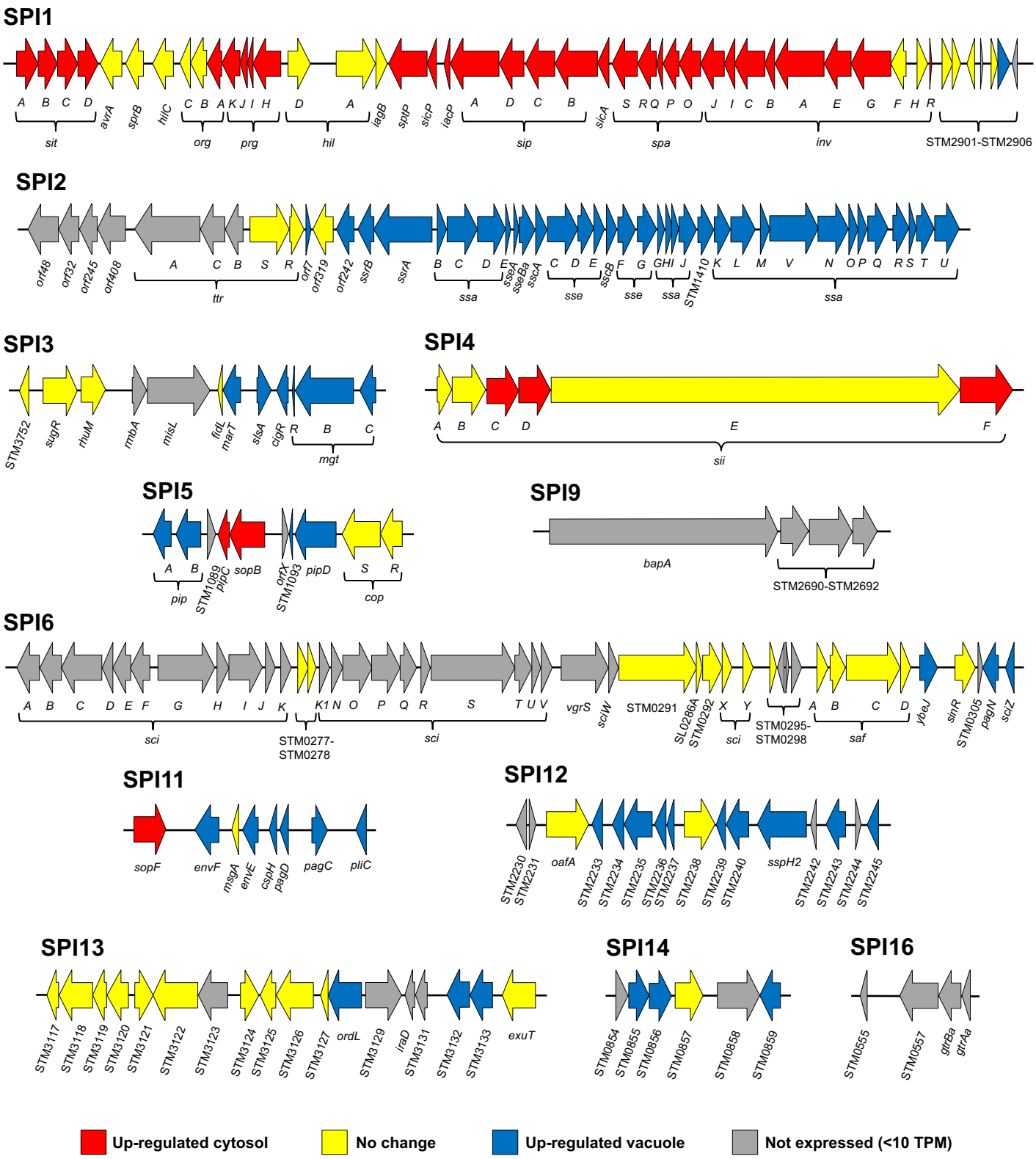

Figure S2. Relative expression of the different PAIs of *S*. Typhimurium. Each arrow represents an individual gene to scale within each PAI. The different islands are also scaled against each other. The color of each arrow represents relative gene expression – red arrows depict genes up-regulated in the cytosol (≥1.40-fold change WTM/EBSS), blue are genes up-regulated in the vacuole (≤0.71-fold change WTM/EBSS), yellow are genes with unchanged expression (0.72-1.39-fold change) and grey arrows are genes with a TPM value <10 and considered not expressed. See Dataset S1 for the entire data set. Adapted from Srikumar et al. (41)

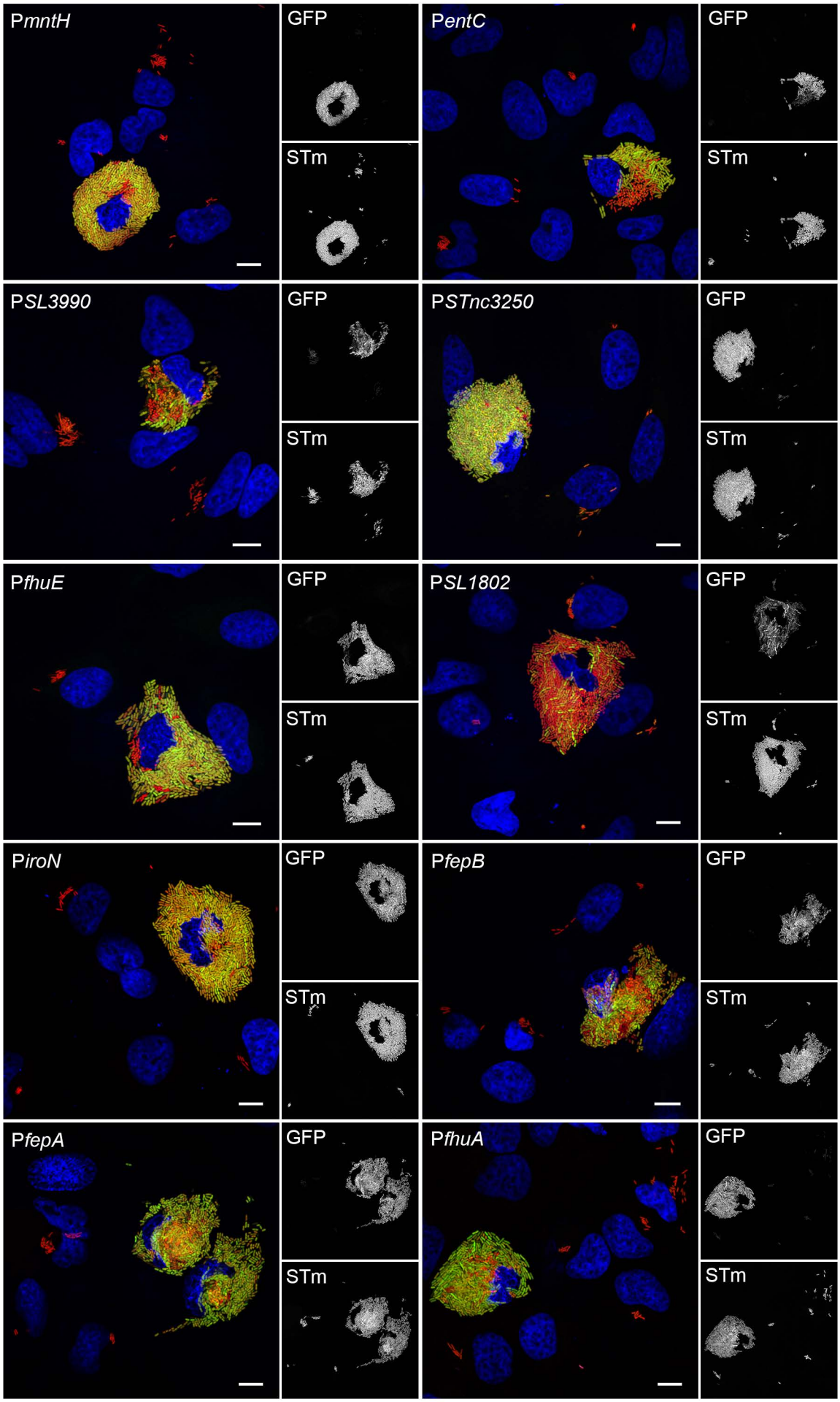

Figure S3. Additional iron-associated genes/sRNAs that are cytosol-specific. Epithelial cells were infected with mCherry-*S*. Typhimurium harboring *gfpmut3* transcriptional reporters. At 8 h p.i., cells were fixed and stained with Hoechst 33342 to detect DNA. Representative confocal microscopy images show induction of *mntH*, *entC*, SL3990, STnc3250, *fhuE*, SL1802, *iroN*, *fepB*, *fepA* and *fhuA* promoters in cytosolic bacteria. Green = transcriptional reporter, red = *S*. Typhimurium, blue = DNA. Scale bars are 10 µm.

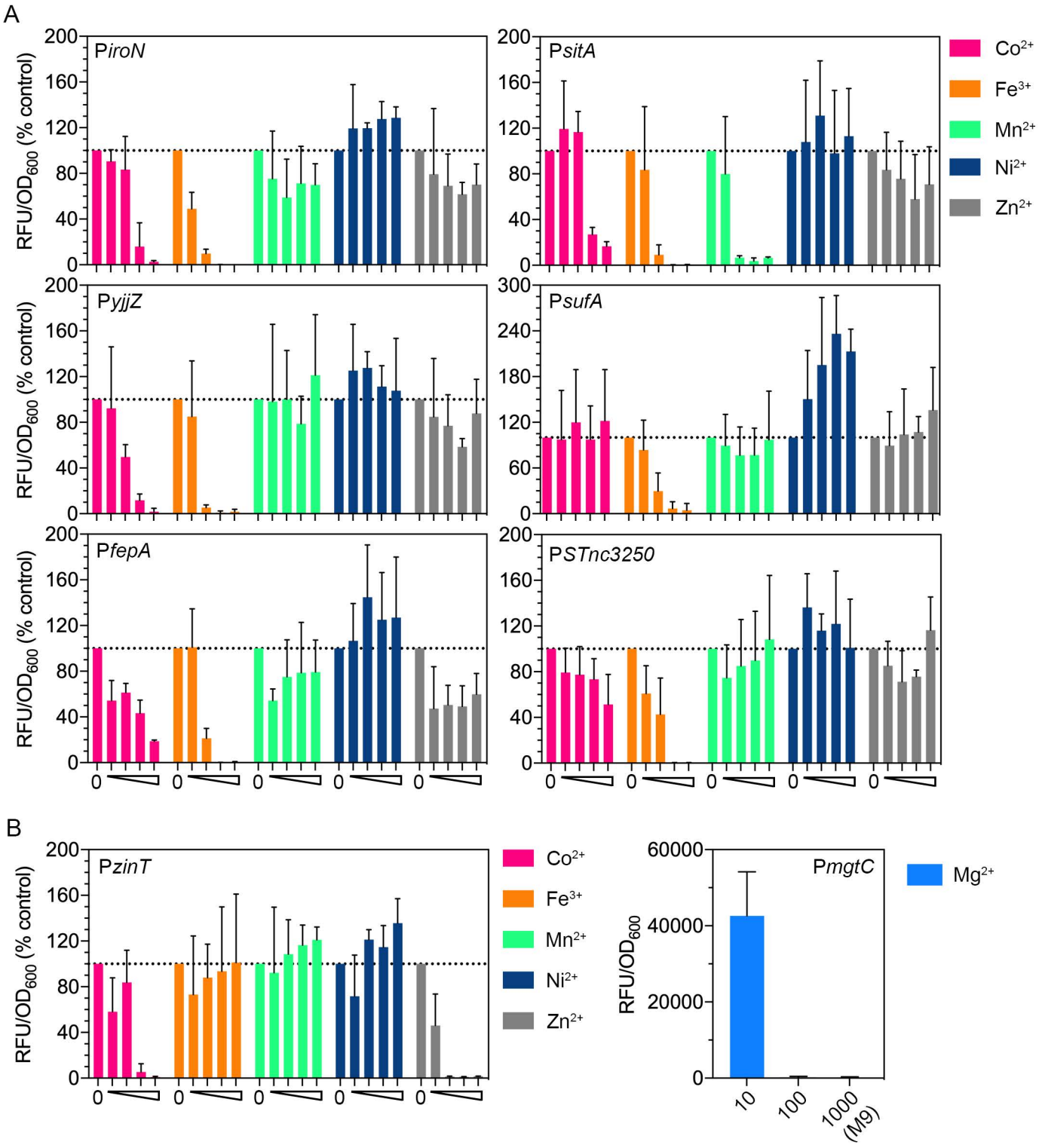

Figure S4. The common metal regulator of cytosol-specific gene/sRNA transcription is iron. (A). GFP fluorescence in mCherry-S. Typhimurium harboring P*iroN-gfpmut3*, P*sitA-gfpmut3*, P*yjjZ-gfpmut3*, P*sufA-gfpmut3*, P*fepA-gfpmut3* or P*STnc3250-gfpmut3* reporter plasmids. Bacteria were grown shaking overnight at 37°C for 16 h in M9-supplemented media containing increasing concentrations of $CoCl_2$, $FeCl_3$, $MnCl_2$, $NiCl_2$ or $ZnCl_2$ (0.1 μM, 1 μM, 10 μM or 100 μM). No added cation (0) served as the control. The relative fluorescence units (RFU) were normalized to OD_{600} and expressed as a percentage of control. Background GFP fluorescence of mCherry-*S*. Typhimurium (no reporter) was subtracted from all values. n≥3 independent experiments. (B) GFP fluorescence in mCherry-*S*. Typhimurium harboring P*zinT-gfpmut3* or P*mgtC-gfpmut3* plasmids. Growth and analysis of *zinT* expression was as described in (A).Standard M9 minimal media contains 1 mM $MgSO_4$ which completely represses *mgtC* expression. The effect of Mg^{2+} concentration on *mgtC* expression was therefore assessed in M9-supplemented media containing decreasing amounts of $MgSO_4$ i.e. 1000 μM (standard), 100 μM and 10 μM. Mg^{2+} concentrations lower than 10 μM considerably impacted bacterial growth. n=3 independent experiments.

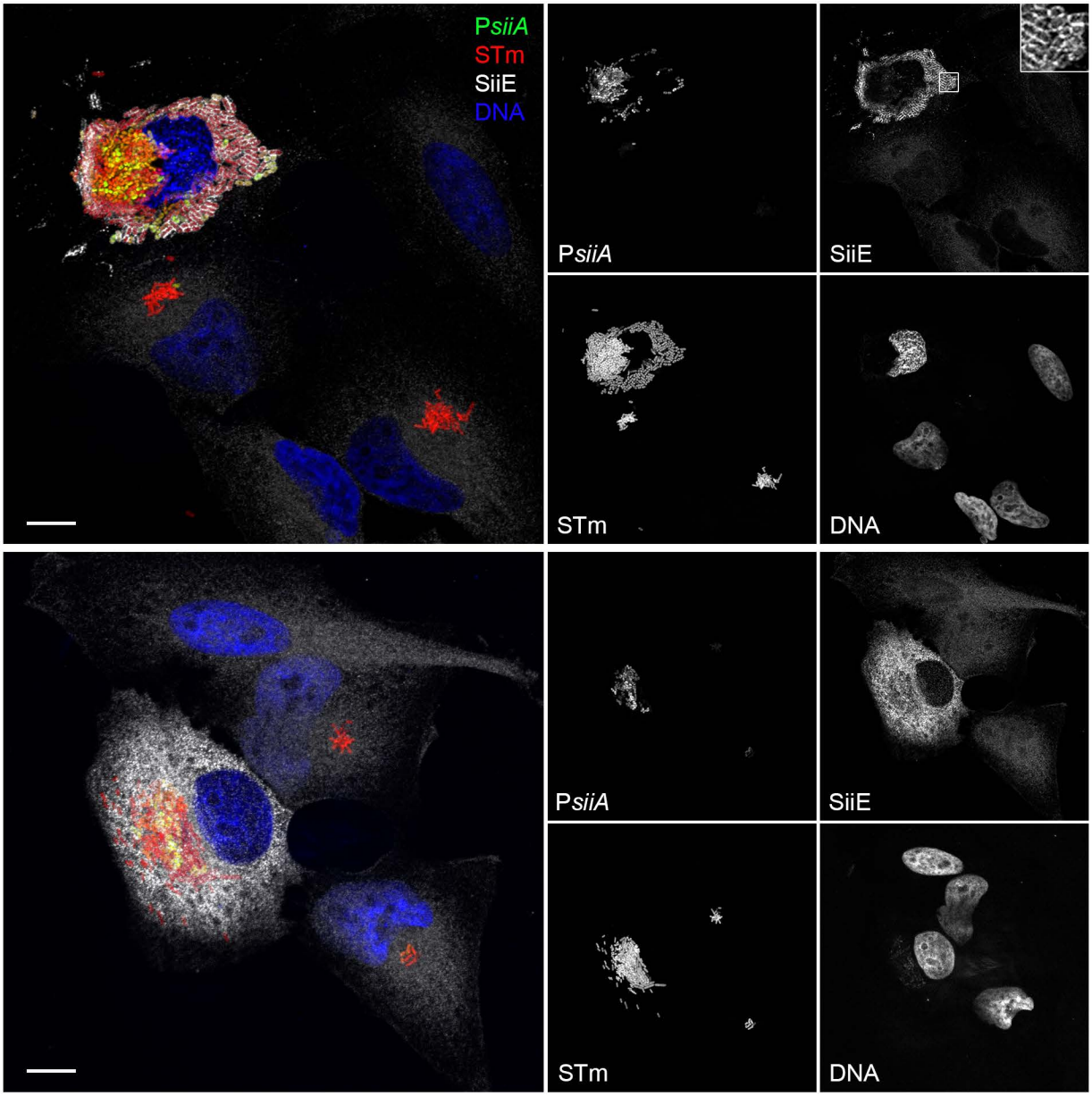

Figure S5. Cytosolic bacteria produce SiiE. Epithelial cells seeded on coverslips were infected with mCherry-*S*. Typhimurium harboring a P*siiA-gfpmut3* transcriptional reporter. At 8 h p.i., cells were fixed and immunostained with polyclonal antibodies directed against SiiE. DNA was stained with Hoechst 33342. Representative confocal microscopy images show SiiE attached to (upper panel) or secreted by (lower panel) cytosolic bacteria. Inset shows enlargement of boxed area. Green = P*siiA-gfpmut3* reporter, red = *S*. Typhimurium, white = SiiE, blue = DNA. Scale bars are 10 µm.

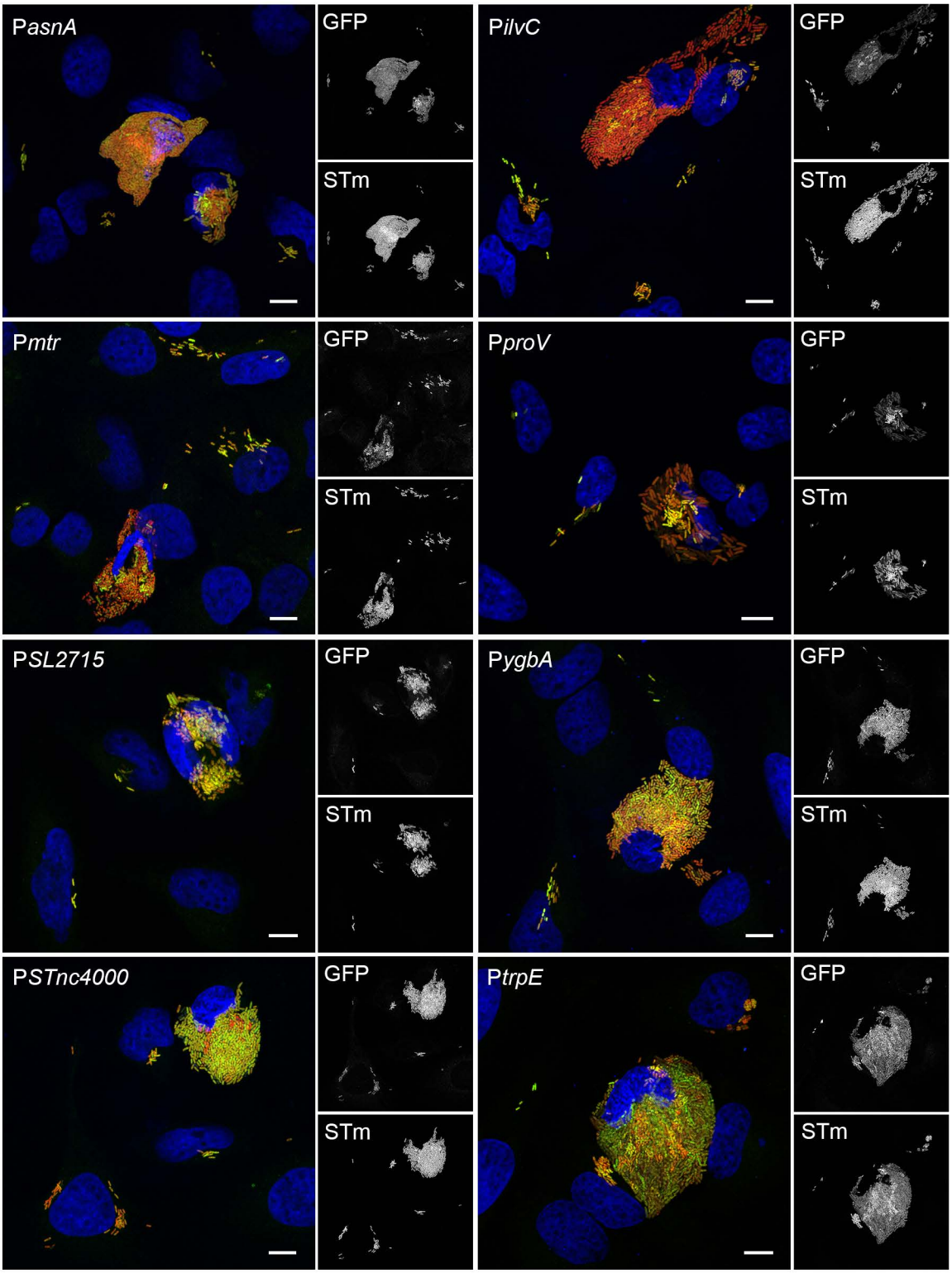

Figure S6. RNA-seq-predicted genes/sRNAs that were not confirmed by transcriptional reporters. Epithelial cells seeded on coverslips were infected with mCherry-*S*. Typhimurium harboring *gfpmut3* transcriptional reporters. At 8 h p.i., cells were fixed and stained with Hoechst 33342 to detect DNA. Representative confocal microscopy images show equivalent expression of *asnA*, *ilvC*, *mtr*, *proV*, SL1344_2715, *ygbA*, STnc4000 and *trpE* promoters in vacuolar and cytosolic bacteria. Green = transcriptional reporter, red = *S*. Typhimurium, blue = DNA. Scale bars are 10 µm.

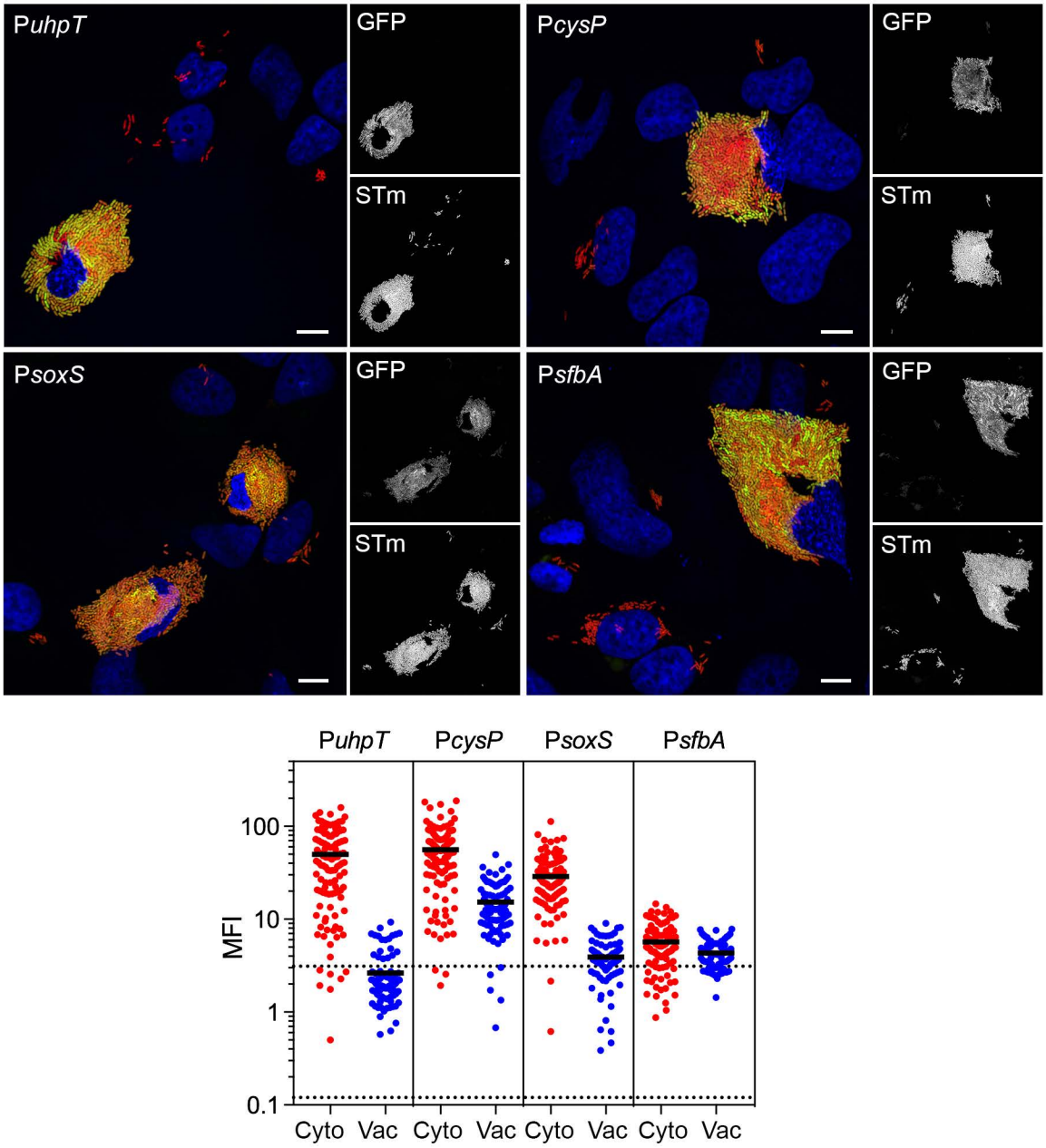

Figure S7. Identification of additional *S*. Typhimurium genes that are up-regulated in the epithelial cytosol. Upper panels: Epithelial cells seeded on coverslips were infected with mCherry-*S*. Typhimurium harboring *gfpmut3* transcriptional reporters. At 8 h p.i., cells were fixed and stained with Hoechst 33342 to detect DNA. Representative confocal microscopy images show induction of *uhpT, cysP*, *soxS* and *sfbA* promoters in cytosolic bacteria. Green = transcriptional reporter, red = S. Typhimurium, blue = DNA. Scale bars are 10 µm.
Lower panel: Quantification of the MFI of GFP signal in individual bacteria. Bacteria were designated as being cytosolic (Cyto) or vacuolar (Vac) if residing within cells with ≥100 bacteria or 2-40 bacteria, respectively. Each dot represents one bacterium; the solid black line indicates the mean. Acquisition parameters (acquisition time and gain) were set-up using P*cysP-gfpmut3* (the highest GFP signal intensity) and these same parameters were applied throughout. The MFI for each bacterium was determine using ImageJ. Dashed lines indicate the range of background fluorescence in the GFP channel measured for mCherry-*S*. Typhimurium (no reporter). n=2 independent experiments.